Localized waves in inhomogeneous media

A. Vl. Gurevich and R. G. Mints

Institute of High Temperatures, Academy of Sciences of the USSR, Moscow
Usp. Fiz. Nauk **142**, 61–98 (January 1984)

This review examines the localization of one-dimensional nonlinear waves in an inhomogeneous multiphase medium. Particular attention is devoted to the localization of two types of waves, namely, solitary waves (domains) and switching waves that are the separation boundaries between the corresponding phases (domain walls). The localized state of such waves on both point and slowly-varying (in space) inhomogeneities is investigated. It is shown that several types of waves can become localized on inhomogeneities, and variation of external parameters may be accompanied by abrupt transitions between different types of localized waves. The stability of waves localized on inhomogeneities is examined together with various hysteresis phenomena that may occur in an inhomogeneous medium. The general results presented in the first part of the review are illustrated by examples of different physical systems, including superconductors, normal metals, semiconductors, plasmas, and chemical-reaction waves.

CONTENTS

1. INTRODUCTION

The properties of various types of nonlinear waves are being intensively investigated at present. Such waves usually constitute the reaction of a medium to a sufficiently strong external influence, or they arise spontaneously as a result of some instability, for example, in active media that are remote from the state of thermodynamic equilibrium.[1–3] Under certain conditions, this instability may give rise to self-organization, i.e., to the appearance of spatially-inhomogeneous stationary structures.[4–6]

Considerable advances have been achieved in recent years in our understanding of the properties of nonlinear waves in homogeneous media and, in particular, solitary waves, i.e., domains[1)] (Fig. 1a), "domain wall"-type waves (Fig. 1b), and so on. Very powerful mathematical methods have been developed that can often be used to describe not only the static properties of nonlinear waves, but also the dynamics of their interaction with one another (see, for example, Refs. 9 and 10).

Less attention has been devoted to the question of the behavior of nonlinear waves in inhomogeneous media (see, for example, Ref. 11), their localization and stability, and the dependence of the properties of a wave localized on an inhomogeneity on the parameters of the medium, external fields, and so on. It is usually more or less obvious that a traveling nonlinear wave can be trapped by a sufficiently strong inhomogeneity (see, for example, Refs. 8 and 12). This localization (pinning) can result in a substantial change in the properties of the medium. For example, this applies to the change in the current-voltage characteristic (CVC) on pinning, vortices in wide Josephson contacts,[13–16] slow Gunn domains that arise, for example, during recombinational instability in semiconductors,[17,18] resistive domains in superconductors,[19–24] charge-density waves in quasi-one-dimensional compounds,[25,26] and so on.

Usually considerably more attention is devoted to the phenomenon itself of localization of a wave on an inhomoge-

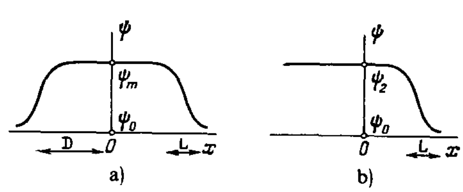

FIG. 1. The distribution $\psi(x)$ for a domain (a) and a "domain wall" (b).

[1)]Such waves are customarily referred to as solitons if, after a sufficient time following their interaction with one another, they retain the shape and velocity they had prior to interaction (see, for example, Refs. 7 and 8).

 0038-5670/84/010019-23$01.80

neity and the conditions necessary for its appearance than to the properties of the localized wave as such. On the other hand, even a relatively weak inhomogeneity can give rise to an appreciable change in the parameters of a wave localized upon it and, in particular, to the stabilization of a wave that is unstable in a homogeneous medium, and also to the appearance of qualitatively new types of localized waves. The possibility of localization of nonlinear waves on inhomogeneities may give rise to a great variety of hysteresis phenomena in superconductors,[15,16,22–24,27,28] in semiconductors (see, for example, Refs. 18 and 19) and semiconductor structures,[30] in low-temperature plasmas,[31] and in many biological systems.[32,33] It may also give rise to characteristic anomalies during phase transitions,[34,35] and so on. The present review is devoted to the presentation, from a unified point of view, of the theory of nonlinear waves localized on inhomogeneities.

We shall consider systems in which these waves can be described by the single nonlinear equation

$$\frac{\partial}{\partial t}\,\mu\,\frac{\partial\psi}{\partial t}+\nu\,\frac{\partial\psi}{\partial t}=\frac{\partial}{\partial x}\,\varkappa\,\frac{\partial\psi}{\partial x}-q\,\frac{\partial\psi}{\partial x}-f\,(\psi), \qquad (1.1)$$

where μ, ν, $\varkappa$, q, and f are functions of the variable ψ (and of the coordinate x in an inhomogeneous medium). When the functions μ, ν, $\varkappa$, q and f are suitably chosen, this equation describes nonlinear waves encountered in many physical systems, such as Gunn domains in semiconductors[17,18] (ψ is the electric field), various types of thermal waves (ψ is the temperature) in superconductors,[36–38] in normal metals,[39–43] in semiconductors,[17,18,29,64] in liquid helium,[44] in low-temperature plasmas,[31,45–48] in combustion in gaseous mixtures,[49,50] in chemical reactions occurring on the surface of a solid catalyst,[51,52] in concentration waves (ψ is the concentration of atoms or active centers), in alloys[53] and autocatalytic chemical reactions,[49,50,54] in vortices in Josephson junctions,[13] in antiphase domains in quasi-one-dimensional compounds[26] and systems with electron-hole pairing[55,56] (ψ is the phase of the order parameter), in local oscillations near crystal-lattice defects,[57–59] in systems of interacting atoms on a periodic substrate[60,61] (ψ is the displacement of an atom), in nonlinear waves occurring in nonequilibrium superconductors[62] (ψ is the modulus of the order parameter, or the concentration of quasiparticles), in metal-dielectric transitions,[63] and so on.

It is thus clear that we shall be considering a fairly wide range of physical phenomena described by an equation of the same form. This similarity of description leads to a number of specific features that are characteristic for waves localized on inhomogeneities, independently of their specific nature. We shall concentrate on these general features and consider the localization of domains (Fig. 1a) and domain walls (Fig. 1b) on isolated inhomogeneities. Our main interest will be in the physical consequences that ensue from this. The most important relationships will therefore be illustrated by various examples and analogies at the "physical level of rigor." The justifications of these analogies can be found in the various publications to which reference is made throughout this review.

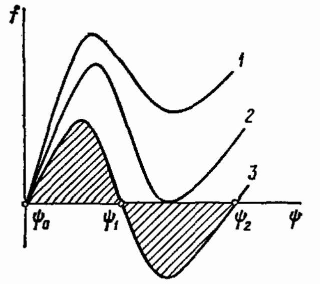

FIG. 2. The function $f=f(\psi)$ for different values of β: 1) $\beta<\beta_1$, 2) $\beta=\beta_1$, 3) $\beta=\beta_p>\beta_1$.

2. NONLINEAR QUASISTATIONARY WAVES

A. Waves in a homogeneous medium

In this section, we shall reproduce the results of the theory of stationary self-preserving waves $\psi=\psi(x-vt)$, propagating in a homogeneous medium with constant speed v, which we shall use in the ensuing account. For simplicity, we shall confine our attention to the nonlinear diffusion equation ($\mu=0$), in which case (1.1) will assume the following form in the coordinate frame moving together with the wave:

$$\frac{d}{dx}\,\varkappa\,\frac{d\psi}{dx}+(\nu v-q)\,\frac{d\psi}{dx}-f\,(x)=0. \qquad (2.1)$$

In most of the cases mentioned in the Introduction, the dependence on ψ is N-shaped, as illustrated in Fig. 2 (examples are: semiconductors with negative differential conductivity,[17,18] superconductors with transport current,[19,20,37,38] chemical chain reactions in "cold" combustion,[49,50] plasmas,[31,45–48] and so on).

The function $f(\psi)$ depends on external parameters. These parameters can be, for example, current, illumination intensity, initial concentration of chemical reagents, rate of plastic deformation, and so on. We shall confine our attention to the simplest case, where the totality of external conditions can be described by introducing the single parameter β, which will thus characterize the strength of external influences on the system. A typical shape of $f=f(\psi,\beta)$ is shown in Fig. 2. When $\beta<\beta_1$, the equation $f(\psi,\beta)=0$ has the single root $\psi=\psi_0$, whereas, for $\beta>\beta_1$, it has three roots: $\psi=\psi_0$, $\psi=\psi_1$, $\psi=\psi_2$. Consequently, when $\beta>\beta_1$, the system can be in one of three homogeneous states. When $\varkappa>0$, $\nu>0$, the states for which $\partial f/\partial\psi>0$ (Fig. 2) are stable under small perturbations $\delta\psi\sim\exp(\lambda t+ikx)$, and the maximum growth rate $\delta=\operatorname{Re}\lambda(k)$ occurs for $k=0$ (see, for example, Ref. 17). Thus, when $\beta>\beta_1$, the states $\psi=\psi_0$ and $\psi=\psi_2$ are stable and can coexist, at least in principle, in the form of two phases with the boundaries (domain walls) between them either at rest or moving.

To describe inhomogeneous distributions $\psi=\psi(x,t)$ corresponding to the two-phase region (Fig. 1), we must examine the corresponding solutions of (2.1). This problem has been solved in many papers for different physical, chemical, and biological systems.[17,18,49,50,65–68] Here, we shall employ a qualitative classification of inhomogeneous solutions $\psi=\psi(x)$, which provides a graphic description of the phenomenon and is based on the formal analogy between (2.1) and the equation of motion of a particle of mass $\varkappa$, where, in

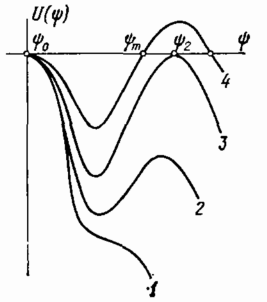

FIG. 3. The "potential energy" $U = U(\psi)$ for different values of β: 1) $\beta < \beta_1$, 2) $\beta_1 < \beta < \beta_p$, 3) $\beta = \beta_p$, 4) $\beta > \beta_p$.

general, this mass depends on the coordinate ψ in the presence of potential energy $U = -S(\psi)$ and frictional force $(\nu v - q)\mathrm{d}\psi/\mathrm{d}x$, and x plays the role of time. If we multiply (2.1) by $\varkappa \mathrm{d}\psi/\mathrm{d}x$ and integrate with respect to x, we obtain

$$S(\psi) = \int_{\psi_0}^{\psi} \varkappa f \,\mathrm{d}\psi. \qquad (2.2)$$

Figure 3 shows the potential "energy" $U = U(\psi)$ corresponding to the "force" $f(\psi)$ of Fig. 2. Bounded solutions $\psi(x)$ correspond to finite particle trajectories in the potential "well" $U = U(\psi)$. Clearly, such trajectories arise only for $\beta > \beta_1$ and the corresponding solution $\psi = \psi(x)$ describes self-preserving waves of finite amplitude. The following types of such waves are possible:

1) Domain wall (Fig. 1b). This solution corresponds to a "trajectory" $\psi = \psi(x)$, on which the particle leaves one maximum of the potential $U = U(\psi)$ with zero initial velocity, and then enters another maximum of $U = U(\psi)$, again with zero velocity. The necessary condition for such solutions is that the energy difference $\Delta U = S(\psi_0) - S(\psi_2)$ must be compensated by the work done by friction $(\nu v - q)\mathrm{d}\psi/\mathrm{d}x$, and this determines the velocity v of the domain wall:

$$\int_{-\infty}^{\infty} (\nu v - q)\,\varkappa \left(\frac{\mathrm{d}\psi}{\mathrm{d}x}\right)^2 \mathrm{d}x = S[\psi(\infty)] - S[\psi(-\infty)], \qquad (2.3)$$

where (and henceforth) we assume, to be specific, that $\psi(-\infty) = \psi_2$ and $\psi(\infty) = \psi_0$ (Fig. 1b).

There is a large number of systems for which q is small $[qL \ll \varkappa$, $(L \sim [\varkappa^{-1}\partial f/\partial\psi]_{\psi_0}^{-1/2}$ is the characteristic spatial scale of variation in $\psi(x)$; cf. Fig. 1]; in particular, they include a great majority of the examples enumerated in the Introduction. As a rule, the fact that q is small does not modify the qualitative aspects of the phenomena under consideration, but enables us to simplify quite substantially our presentation. For this reason, we shall always assume that $q = 0$ unless the finite size of q leads to essentially new effects.

It is clear from Fig. 3 and (2.3) ($q = 0$) that $v > 0$ for $\beta > \beta_p$, and $v < 0$ when $\beta < \beta_p$. The quantity β_p is determined from the equations that constitute the so-called "theorem of equal areas" (see, for example, Refs. 17, 18, 37, 48):

$$f(\beta_p, \psi_2) = 0, \quad S(\beta_p, \psi_2) = 0 \qquad (2.4)$$

(when $\varkappa = \text{const}$, we have the case where the two shaded areas in Fig. 2 are equal).

For $|\beta - \beta_p| \ll \beta_p$, for which v is small, the derivative $\mathrm{d}\psi/\mathrm{d}x$ in (2.3) can be calculated by using the solution $\psi = \psi(x)$ describing the static domain wall. We then have[17,18,37]

$$v = -S(\psi_2)\left(\sqrt{2}\int_{\psi_0}^{\psi_2} \nu \sqrt{S}\,\mathrm{d}\psi\right)^{-1} \sim v_0 \frac{\beta - \beta_p}{\beta_p}, \qquad (2.5)$$

where

$$S(\psi_2) \approx (\beta - \beta_p)\frac{\partial}{\partial\beta} S(\beta, \psi_2)\,|_{\beta_p},$$

and

$$v_0 \sim \frac{L}{\tau}$$

have the dimensions of velocity and consist of the scales of length L and time $\tau \sim \nu L^2/\varkappa$ that are characteristic for this problem.

Thus, the domain wall is a switching wave that takes the system from one stable state $\psi = \psi_0$ to another $\psi = \psi_2$ or vice versa (depending on the magnitude of β). A change in the sign of the velocity of this wave for $\beta = \beta_p$ is an indication of the metastability of homogeneous states with $\psi = \psi_2$ for $\beta_1 < \beta < \beta_p$ and with $\psi = \psi_0$ for $\beta > \beta_p$. In point of fact, when a strong external perturbation produces in the specimen a sufficiently large region in which $\psi \simeq \psi_2$, then, in accordance with the foregoing, this region will expand for $\beta > \beta_p$ and collapse for $\beta < \beta_p$. Similarly, a large enough region with $\psi \simeq \psi_0$ imbedded in the "phase" $\psi = \psi_2$ will expand for $\beta_1 < \beta < \beta_p$ and collapse for $\beta > \beta_p$.

2) Soliton wave–domain (Fig. 1a). This solution may be looked upon as two domain walls separated by a distance $2D$ from one another (see Fig. 1a). The domain corresponds to a trajectory $\psi = \psi(x)$ in the potential $U(\psi)$ (see Fig. 3) on which the particle leaves the point $\psi = \psi_0$ with zero initial velocity, then approaches the point $\psi = \psi_m$, turns around, and returns with zero velocity. This solution describes a "strong field" domain (the term is borrowed from the theory of semiconductors with negative differential conductivity,[17,18] since $\psi(x) > \psi_0$ everywhere in the interior of the domain), and exists only for $\beta > \beta_p$. If, on the other hand, $\beta_1 < \beta < \beta_p$, we have the possibility of a "weak field" domain for which $\psi(x) < \psi_2$, $\psi(\pm\infty) = \psi_2$. This corresponds to the situation where the particle begins and ends its motion at the point $\psi = \psi_2$ with zero velocity. Another condition for the existence of domain solutions is that the work done by the force of friction along the corresponding trajectory $\psi = \psi(x)$ is equal to zero. As a result, the domain is at rest for $q = 0$, but moves with velocity $v \propto q/\nu$ when $q \neq 0$.[17,18]

The domain length $2D$ (Fig. 1a) in the region where $\beta > \beta_p$ is, generally speaking, of the order of L. The exception is the case where $\beta \to \beta_p$. It is readily shown that, if we can write $S(\psi) = S(\psi_2) + b(\psi - \psi_2)^2$ for $\psi \simeq \psi_2$, then $D(\beta) \propto -L \ln[(\beta - \beta_p)/\beta_p]$, i.e., the domain can be looked upon as two domain walls with weak mutual interaction for $\beta \to \beta_p$.

3) Periodic structure. This solution, which may be looked upon as a sequence of "strong field" domains, corresponds to the oscillation of a particle in a potential well $U = U(\psi)$ (cf. Fig. 3).

The stability of the types of waves considered above is, of course, unrelated to the stability of particle trajectories in the potential $U = U(\psi)$. Obviously, this must be investigated separately, using the dynamic equation (1.1). The corresponding analysis (see, for example, Refs. 17, 18, and 65–68) shows that only the domain wall is stable in the regime in which the parameter β is fixed.

B. Waves in an inhomogeneous medium (qualitative analysis)

Let us now consider what happens to the results given in the last section when inhomogeneities are present in the medium. For greater clarity, we shall confine our attention to the solutions of the nonlinear thermal conduction equation

$$\nu \frac{\partial T}{\partial t} = \frac{\partial}{\partial x} \varkappa \frac{\partial T}{\partial x} - f(T), \tag{2.6}$$

where ν is the specific heat, $\varkappa$ is the thermal diffusivity $f = W - Q$, $Q(T)$ is the specific heat release, $W = h(T)(T - T_0)/d$ is the rate of loss of heat to the coolant at temperature T_0, $h(T)$ is the heat transfer coefficient, $d = A/P$, A is the area, and P is the perimeter of the cross section of the specimen.

The equation given by (2.6) describes a broad range of nonequilibrium phenomena that arise when a medium is heated by an electric field, by chemical reactions, by plastic deformation, and so on. When the cross section of the specimen is small, or when little heat is given up to the coolant ($dh \ll \varkappa$), Eq. (2.6) gives the temperature $T(x,t)$ averaged over the transverse cross section (the y,z plane). Equation (2.6) may also include a term of the form $-q\, \partial T/\partial x$, which is due to, for example, the Thomson heat[69] that is small in comparison with Q.

If the waves in which we are interested are to exist in a homogeneous medium, we must ensure that the heat balance equation $Q(T) = W(T)$ is satisfied for a number of temperatures. This situation is frequently encountered when phase transitions occur in the system in relatively narrow temperature intervals, or when the functions $Q(T)$ or $W(T)$ are N- or S-shaped, and so on. Figure 4 illustrates some characteristic cases. For example, Fig. 4a corresponds to a phase transition, at $T = T_c$, from a highly conducting to a poorly conducting state in the presence of a heating transport current, and Fig. 4b illustrates the appearance of three crossing points for $Q(T)$ and $W(T)$ that appear because of the N-shaped form of $W(T)$, which often arises when there is a large heat flow from the specimen to the coolant.[70,71] The S-shaped $Q(T)$ frequently occurs in gases or semiconductor plasmas in strong electric fields.[72–74] Three crossing points

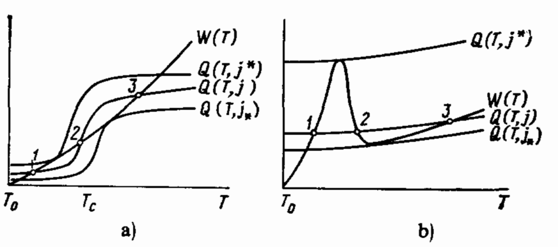

FIG. 4. Characteristic shapes of $Q(T)$ and $W(T)$ for a phase transition (a) and boiling crisis of coolant (b) in the case of Joule heating of a conductor by a current of density in the range $j_* < j < j^*$.

may also occur for $Q(T)$ and $W(T)$ in the case of second-order phase transitions, for example, antiferromagnetic transitions in metals that lead to anomalies in the resistivity $\rho(T)$.[39,43]

In the heat-transfer problem that we are considering, the inhomogeneity in the medium has a simple physical interpretation: it is due to the presence of a region of increased (reduced) heat release or heat removal. We now proceed to the case of waves (domains and domain walls) that are localized ($\partial T/\partial t = 0$) on an inhomogeneity. Equation (2.6) cannot be solved for $\partial T/\partial t = 0$ and arbitrary dependence of f and $\varkappa$ on T and x. We shall therefore confine our attention to two limiting cases, namely, a point inhomogeneity ($\varepsilon \gg 1$) and a continuous inhomogeneity ($\varepsilon \ll 1$). The parameter

$$\varepsilon = \frac{L}{l} \tag{2.7}$$

is the ratio of the characteristic spatial scale $L \propto \sqrt{d\varkappa/h}$ of changes in the temperature $T(x)$ to the size l of the inhomogeneity.

We begin with $\varepsilon \gg 1$, for which the inhomogeneity may be looked upon as a point source (sink) of heat.[22] Equation (2.6) then becomes

$$\frac{d}{dx} \varkappa \frac{dT}{dx} - f(T) + F(T)\,\delta(x) = 0, \tag{2.8}$$

where $F \sim \Delta f\, l$, and Δf is the characteristic change in $f(T,x)$ in the interior of the inhomogeneity [the specific form of $F(T)$ is unimportant in this case].[2)] Equation (2.8) admits of a simple mechanical interpretation: it describes the potential motion of a particle which, at "time" $x = 0$, experiences a shock that communicates to it an additional momentum $F(T_m)$ at the point $T_m \equiv T(0)$. An important point for our analysis will be that T_m determines uniquely the particle trajectory,[75] i.e., the solutions $T = T(x)$ that are of interest to us.

1) Domain ($\varepsilon \gg 1$). For a domain, we have, by virtue of symmetry, $T(x) = T(-x)$. This is equivalent to the elastic reflection of the particles at $T = T_m$ for $x = 0$. Applying the conservation of momentum to this reflection process, we find that

$$\varkappa \frac{dT}{dx}\Big|_{+0} - \varkappa \frac{dT}{dx}\Big|_{-0} = -F(T_m).$$

Using this relation and the conservation of "energy"

$$\frac{1}{2}\left(\varkappa \frac{dT}{dx}\right)^2 = S(T) \tag{2.9}$$

we can readily obtain the equation for T_m in the form[22,23]

$$S(T_m) = \frac{1}{8} F^2(T_m). \tag{2.10}$$

This equation is conveniently investigated by a graphical method. This is done in Fig. 5, which is drawn for $F(T) = \text{const}$. The solid line represents the function $S(T)$ and broken line $F^2/8$. The presence of several crossing points corresponds to several types of domain that can be localized on the inhomogeneity.

We must now consider in greater detail the localized "strong field" domains (hot regions in a cold phase). When

[2)]If the transverse size of the inhomogeneity is less than the characteristic transverse size d of the specimen, the expression for F must be averaged over the cross section of the specimen.

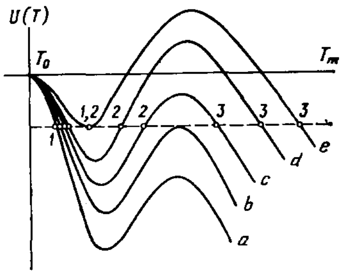

FIG. 5. Graphical solution of (2.10) for different cases: a-$\beta<\beta_r$, b-$\beta=\beta_r$, c-$\beta_r<\beta<\beta_p$, d-$\beta_p<\beta<\beta_k$, e-$\beta=\beta_k$.

$F>0$ (enhanced heat release in the inhomogeneity), we then have

$$\left.\frac{dT}{dx}\right|_{+0}<0, \quad T_m=\max T(x)$$

(Fig. 6a). The graphical analysis given in Fig. 5 clearly shows that, when $\beta<\beta_p$, three different types of domain can become localized on the inhomogeneity, and two can be so localized for $\beta>\beta_p$. The last conclusion is connected with the fact that conservation of energy prevents the particle from reaching the crossing point 3.

When $F<0$ (reduced heat release on the inhomogeneity), we have $dT/dx|_{+0}>0$ and the nature of the trajectories $T(x)$ in which we are interested undergoes a change because T_m is now no longer the maximum temperature in the domain (Fig. 6b). In this case, the particle begins its motion at $T=T_0$, reaches the crossing point between $S(T)$ and the horizontal axis, and then turns around and is reflected at point 1 or point 2 in Fig. 5. Obviously, such trajectories can exist only for $\beta>\beta_p$.

Thus, the inhomogeneity may give rise to the localization of several types of domain, both for $\beta>\beta_p$ and (this is the most interesting case) for $\beta<\beta_p$, when the "strong field" domain cannot exist in a homogeneous medium.

We shall now discuss the stability of domains localized on inhomogeneities. The points $\beta=\beta_r$ and $\beta=\beta_k$ (see Fig. 5), at which the two types of domain appear (disappear) simultaneously, and coalesce for $\beta=\beta_r$ and $\beta=\beta_k$, respectively, are points of bifurcation[76] of (2.8). It will be shown below that, in the neighborhood of such bifurcation points, the growth rate of the most "dangerous" perturbations is small, and vanishes altogether at the bifurcation points themselves. Thus, the stability of stationary localized domains is violated by infinitesimally small perturbations near $\beta=\beta_r$ and $\beta=\beta_k$. This enables us to deduce the stability criterion in which we are interested from the following simple qualitative considerations.

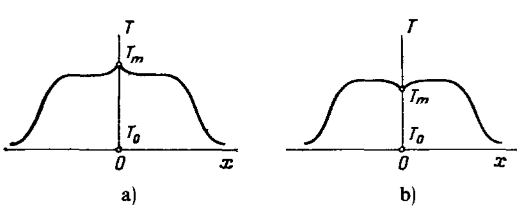

FIG. 6. Temperature distribution in a localized domain for $F>0$ (a) and $F<0$ (b).

Suppose that a weak external influence produces a temperature fluctuation and, consequently, a fluctuation in T_m. The domain will, of course, be stable if an increase in T_m ensures that the total heat $\tilde{W}$ removed from the entire domain exceeds the total heat release $\tilde{Q}$, i.e., $\delta\tilde{f}>0$, where $\tilde{f}=\tilde{W}-\tilde{Q}$. The fluctuation $\delta\tilde{f}$ can be written in the form

$$\delta\tilde{f}=\delta T_m\frac{\partial}{\partial T_m}\left[\int_{-\infty}^{\infty}(W-Q)\,dx-F(T_m)\right],$$

so that the stability condition for a localized domain assumes the form

$$\frac{\partial}{\partial T_m}\int_{-\infty}^{\infty}f\,dx>\left.\frac{\partial F}{\partial T}\right|_{T_m}. \tag{2.11}$$

If we use energy conservation (2.9), the equation given by (2.10), and the relation $\varkappa f=\partial S/\partial T$, we can rewrite the left-hand side of the inequality given by (2.11) in the form

$$\frac{\partial}{\partial T_m}\int_{-\infty}^{\infty}f\,dx=\frac{\partial}{\partial T_m}\int_{T_0}^{T_m}\varkappa f\sqrt{\frac{2}{S}}\,dT=\left(\varkappa f\sqrt{\frac{2}{S}}\right)_{T_m}$$
$$=\frac{4}{F(T_m)}\left.\frac{\partial S}{\partial T}\right|_{T_m}.$$

As a result, we obtain the stability condition for a domain localized on an inhomogeneity (for a given value of β) in the form[23]

$$F\frac{\partial}{\partial T}\left(S-\frac{F^2}{8}\right)\Big|_{T_m}>0. \tag{2.12}$$

It follows from (2.12) that, if the solution is stable, then $\partial T_m/\partial\beta>0$, i.e., the temperature of the inhomogeneity increases with increasing parameter β that characterizes the external influence. Physically, this condition is fairly obvious.

The inequality given by (2.12) signifies that, if the domain is stable, the slope of the graph of $S(T)$ at the point $T=T_m$ is greater than the slope of the graph of $F^2(T)/8$. In our specific example (see Fig. 5), the crossing points 1 and 3 correspond to stable domains. Crossing point 2 (see Fig. 5) corresponds to an unstable domain. As $F\to 0$, this domain will go over to the domain in a homogeneous medium that was discussed in the last section.

The domain at temperature T_m that corresponds to point 1 in Fig. 5 arises in connection with the local heating by the inhomogeneity ($F>0$) of the original stable homogeneous state $T=T_0$. As far as the domain for which T_m corresponds to point 3 in Fig. 5 is concerned, its appearance is connected with the stabilization by the inhomogeneity of a region of hot phase with $T=T_2$. It is clear from Fig. 5 that this type of domain will exist for $\beta_r<\beta<\beta_p$, where β_r is determined by the following set of equations:[22,23]

$$\begin{cases} S(T_m,\beta_r)=\dfrac{F^2}{8}(T_m,\beta_r), \\ \dfrac{\partial}{\partial T}\left[S(T,\beta_r)-\dfrac{F^2}{8}(T,\beta_r)\right]_{T_m}=0. \end{cases} \tag{2.13}$$

As $\beta\to\beta_r$, the solutions of (2.8) that correspond to points 2 and 3 in Fig. 5 coalesce into one, which vanishes abruptly for $\beta<\beta_r$. When this happens, $\delta\beta\equiv\beta_p-\beta_r\sim F^2(\partial S/\partial\beta)$ or

$$\frac{\delta\beta}{\beta_p} \sim \frac{F^2}{(T_m - T_0)\varkappa Q} \sim \left(\frac{F}{LQ}\right)^2 \equiv \Gamma^2 \sim \left(\frac{l}{L}\right)^2 \left(\frac{\Delta f}{f}\right)^2, \quad (2.14)$$

where we have taken into account the fact that $Q \sim W$. The ratio $\delta\beta / \beta_p$ may be looked upon as a measure of the effect of the inhomogeneity on the properties of the domain and, as is clear from (2.14), it is determined by the ratio of the heat released in the inhomogeneity, F, and the heat released in the entire domain, LQ. Correspondingly, we can distinguish between strong ($\Gamma \sim 1$) and weak ($\Gamma \ll 1$) coupling between the domain and the inhomogeneity. The estimate given by (2.14) shows that the necessary condition for strong coupling is the presence of a strong ($\Delta f / f \sim \varepsilon \gg 1$) inhomogeneity. If we then consider the example of a medium heated by a current, this situation can arise only for high local current concentrations ($A / A_0 \sim \sqrt{\varepsilon}$, where A_0 is the cross-sectional area of the inhomogeneity), or when there is a large change in the conductivity within the inhomogeneity ($\sigma / \sigma_0 \sim \varepsilon$).

It is clear from Fig. 5 that, as β increases ($\beta \to \beta_k$), the points 1 and 2 coalesce and, when $\beta > \beta_k$, the static domain solutions are absent altogether. Both critical parameters, β_r and β_k ($\beta_k > \beta_r$), are obviously different roots of the same set of equations given by (2.13) (see Fig. 5).

When $\beta > \beta_k$, the presence of the inhomogeneity leads to a local heating of the original metastable state with $T = T_0$, such that the phases cannot coexist and the system goes over to the state with $T = T_2$ or, in other words, the phase with $T = T_0$ is absolutely unstable for $\beta > \beta_k$. The condition $\beta > \beta_k$ is analogous to the condition for the ignition of a fuel mixture on a hot surface (see, for example, Refs. 49 and 50).

Thus, in contrast to the homogeneous medium, where the coexistence of phases with $T = T_0$ and $T = T_2$ is possible only when $\beta = \beta_p$ is strictly satisfied, an inhomogeneous medium can support several types of stable localized domains that appear in the range $\beta_r < \beta < \beta_k$.

The localization of a "weak field" domain can be examined in an analogous manner.

2) Domain wall ($\varepsilon \gg 1$). The trajectory $T = T(x)$ corresponding to a localized domain wall begins at the point $T = T_0$ (see Fig. 5) and ends at $T = T_2$, where the additional momentum F is communicated to the particle so that it changes its energy by the amount $\Delta U = S(T_2) - S(T_0)$, and arrives at $T = T_2$ with zero velocity. Since $\Delta U = S_2 \equiv S(T_2) \propto \mathrm{sign}(\beta_p - \beta)$, for $\beta < \beta_p$ the particle must be retarded on "impact", and for $\beta > \beta_p$ it must be accelerated (see Fig. 5). Hence, it follows that the localized domain wall can exist only for $F > 0$ when $\beta < \beta_p$, and for $F < 0$ when $\beta > \beta_p$.

Let us now examine in greater detail the situation where $F > 0$ ($\beta < \beta_p$). When F is small (see below), the particle will be retarded somewhat as a result of the "impact", but will not change its direction of motion. Such trajectories $T = T(x)$ are shown in Fig. 7a, where the "impact" can occur only for $T_m > T_2$. Using conservation of energy and momentum, we can readily obtain the equation for T_m:

$$\sqrt{2S(T_m)} - \sqrt{2(S(T_m) - S_2)} = F(T_m). \quad (2.15)$$

It is then readily verified that (2.15) can have solutions if $F^2 < 2|S_2|$. As F increases, the particle will experience "inelastic reflection" as a result of the impact, i.e., it will reverse its direction of motion. Such trajectories $T = T(x)$ are shown in Fig. 7b. We note that the impact can now occur both for $T_m > T_2$ and for $T_m < T_2$. Proceeding by analogy with the foregoing, we can readily obtain the equation for the temperature T_m in the form

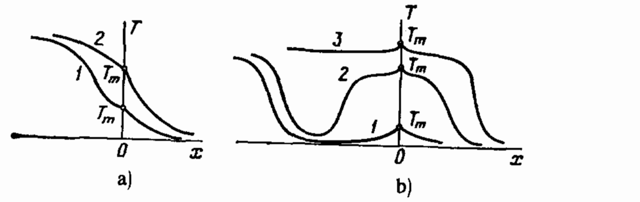

FIG. 7. Temperature distribution in localized domain walls for $F > 0$: a) $\beta_2 < \beta < \beta_3$, b) $\beta_3 < \beta < \beta_p$.

$$\sqrt{2S(T_m)} + \sqrt{2(S(T_m) - S_2)} = F(T_m), \quad (2.16)$$

which can have solutions when $F^2 > 2|S_2|$.

The two relationships given by (2.15) and (2.16) can conveniently be rewritten in the form

$$S(T_m) = R(T_m) \equiv \frac{1}{2}\left[\frac{F(T_m)}{2} + \frac{S_2}{F(T_m)}\right]^2. \quad (2.17)$$

Figure 8 shows a graphical analysis of the solutions of this equation where, for simplicity, we have set $F(T) = \text{const}$. For parameter values for which $F^2 < 2|S_2|$, the solutions in which we are interested correspond to points 1 and 2 (these "trajectories" are shown in Fig. 7a), whereas $2|S_2| < F^2$ corresponds to points 1, 2, and 3 (these "trajectories" are shown in Fig. 7b).

Thus, when $\beta_2 < \beta < \beta_3$, we have two types of domain wall localized on the inhomogeneity. When $\beta_3 < \beta < \beta_p$, there are three such domain walls. Here, β_2 is the minimum value of β for which a nontrivial solution of (2.17) appears, and β_3 is determined from the relation $2|S_2(\beta_3)| = F^2(\beta_3)$.

Near the bifurcation point $\beta = \beta_2$, the two types of domain wall are not very different and, when $\beta = \beta_2$, they go over into each other. This behavior of the solutions in which we are interested signifies (see, for example, Ref. 76) that their stability is due to the way in which slow perturbations develop. Consequently, the stability condition for localized domain walls can be investigated for $\beta_2 < \beta < \beta_3$ by using simple qualitative considerations, similar to those introduced above when localized domains were examined. If we

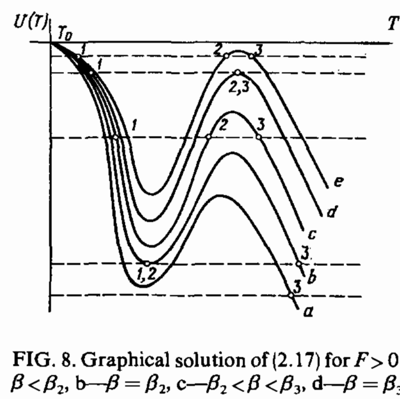

FIG. 8. Graphical solution of (2.17) for $F > 0$ and different values of β: a—$\beta < \beta_2$, b—$\beta = \beta_2$, c—$\beta_2 < \beta < \beta_3$, d—$\beta = \beta_3$, e—$\beta_3 < \beta < \beta_p$.

take into account conservation of "energy" and the equation given by (2.15), we find that the stability condition assumes the form

$$F\frac{\partial}{\partial T}(R-S)\,|_{T_m} > 0. \qquad (2.18)$$

The last inequality signifies that the localized domain wall is stable for $F>0$ if the slope of $R=R(T)$ at $T=T_m$ is greater than the slope of $S=S(T)$. Hence, it follows in particular that, in our example ($F=$ const), the stable domain wall corresponds to point 2 (see Fig. 8), whereas the unstable domain wall corresponds to point 1.

A further (new) solution $T(x)$, which was absent for $\beta<\beta_3$, appears when $\beta_3<\beta<\beta_p$. This is represented by the curve marked 2 in Fig. 7b. The stability criterion for this solution cannot be obtained from the above qualitative considerations because the most "dangerous" perturbation now have nonzero growth rates even at $\beta=\beta_3$.

For a weak inhomogeneity ($\Gamma\ll 1$), the magnitude of β_2 for which the localized domain wall appears for the first time is close to β_p. The parameter β_2 can then be found from (2.17), where we must set $\beta=\beta_p$ everywhere except in the term $S_2/F\propto(\beta_p-\beta_2)$. This yields

$$(\beta_2-\beta_p)\frac{\partial S}{\partial\beta}\bigg|_{\beta_p}\approx F\sqrt{2S(T_1,\beta_p)}\backsim\Gamma.$$

Thus, $\beta_2-\beta_p\sim\Gamma\beta_p$, i.e., when $\Gamma\ll 1$, the domain wall may become localized in a much broader interval of β than the domain [compare with (2.14)].

3) Domain ($\varepsilon\ll 1$). In the case of a smoothly-varying ($\varepsilon\ll 1$) inhomogeneity, all the medium parameters vary slowly over the characteristic length L. If a domain-wall type wave is then excited in the medium, its propagation velocity will vary slowly, depending on the local value of the parameter $\beta_p(x)$ [see Eq. (2.5)], i.e.,

$$\dot{D}=v(D), \qquad (2.19)$$

where D is the coordinate of the domain wall and v is its velocity obtained from (2.5), written locally for each point in the medium.

To be specific, suppose that the domain wall is excited in a region where $\beta>\beta_p(x)$, i.e., the hot phase ($T=T_2$) expels the cold phase ($T=T_0$). If, in the course of its motion, the wave encounters a region in which $\beta<\beta_p(x)$, it will come to rest, and its localized state will be stable. In point of fact, a small deviation δD of the domain wall from the position of equilibrium will, by virtue of (2.19), satisfy the equation

$$\delta\dot{D}=\frac{\partial v}{\partial x}\bigg|_D\delta D. \qquad (2.20)$$

The damping rate of the perturbation $\delta D\propto\exp(\lambda t)$ is given by

$$\lambda=\frac{\partial v}{\partial x}\bigg|_D\backsim-\frac{v_0}{\beta_p}\frac{\partial\beta_p}{\partial x}\bigg|_D, \qquad (2.21)$$

where we have used (2.5). The expression given by (2.21) shows that the localized domain wall is stable ($\lambda<0$) if, for $\partial\beta_p/\partial x>0$, the $T=T_0$ phase lies to the right of the point $x=D$ and the $T=T_2$ phase lies to the left of this point. Otherwise, it is unstable. The reverse situation occurs for $\partial\beta_p/\partial x<0$.

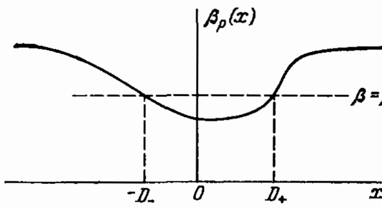

FIG. 9. Determination of the dimensions of a localized domain for $\varepsilon\ll 1$.

Let us now consider a localized domain for $\varepsilon\ll 1$. If the size D of the domain is much greater than the width of its boundaries $\sim L$ (see Fig. 1a), we have two independent domain walls, the motion of each of which being determined by the local $\beta_p(x)$. As an example, consider the case where $\beta_p(x)$ has a minimum (Fig. 9). In accordance with the foregoing, the quantities $D_\pm$ in Fig. 9 can be determined from the equations[24,29]

$$\beta=\beta_p(D_\pm), \qquad (2.22)$$

where $\beta_p(x)$ is found with the aid of the local "equal areas theorem" (2.4). The "strong field" domain localized in the interior of the inhomogeneity shown in Fig. 9 is stable, and its dimensions rise with increasing β.

For $\beta\to\beta_p(0)$ (see Fig. 9), the quantities $D_\pm$ become of the order of L, and (2.22) is no longer valid. When $D\sim L$, the parameters of the medium vary little over the length of the domain and, if $\beta>\beta_p(0)$, we are back to the situation involving a domain in a homogeneous medium. The presence of the inhomogeneity manifests itself only as a slight (proportional to ε^2) deformation of the domain due to the presence of the parabolic well in $\beta_p(x)$.

Thus, for $\varepsilon\ll 1$, two types of domain can become localized on the inhomogeneity. The first exists in the range $\beta_p(0)\lesssim\beta\lesssim\beta_p(\infty)$, has macroscopic (on the scale of L) dimensions, and is stable. The second exists for $\beta\gtrsim\beta_p(0)$ and its dimensions are of the order of L. It has practically indistinguishable properties as compared with the domain in the homogeneous medium, so that it is unstable when the parameter β is fixed.

The presence of a nonmonotonic $\beta_p(x)$, for example, in the case of closely spaced inhomogeneities (Fig. 10), leads not only to the localization of domains, but also to a series of hysteresis phenomena as β increases (decreases). In point of fact, suppose that a "strong field" domain is localized at the center of the deepest well ($x=0$ in Fig. 10). The length of this

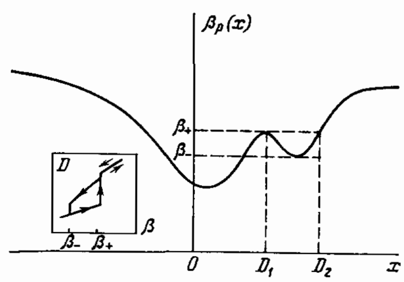

FIG. 10. Localization of a domain in the presence of two smooth inhomogeneities. The corresponding function $D=D(\beta)$ is shown in the insert on the left.

domain increases monotonically with increasing β up to $\beta = \beta_+$. It then abruptly increases at $\beta = \beta_+$ by the amount $D_2 - D_1$ (see Fig. 10), and thereafter again increases monotonically with increasing β.

If we now allow β to decrease, the length of the domain will monotonically decrease, and an "interlayer" of the cold phase with $T = T_0$ will appear in the interior of the domain for $\beta_- < \beta < \beta_+$, the length of which will monotonically increase with decreasing β, so that, for $\beta < \beta_-$, we shall again enter the region in which there is no hysteresis. Thus, hysteresis occurs for $\beta_- < \beta < \beta_+$. This is illustrated by Fig. 10, which also shows the function $D = D(\beta)$ (the nature of the relatively small jumps that occur when β is reduced again will be examined below).

The hysteresis connected with the presence of several inhomogeneities can be detected experimentally in the form of a discontinuous change in the properties of the system for small changes in β and, in particular, in the form of abrupt changes in the current-voltage characteristics, in deformation during plastic flow,[77,78] in absorption of energy under illumination by light, and so on.

We note that experimental determinations of $T = T(x)$ for different β in a specimen containing domains can be used to determine the function $D = D(\beta)$, and hence deduce $\beta_p(x)$. For example, for a parabolic well on $\beta_p(x)$, we obtain

$$D(\beta) \propto \sqrt{\beta - \beta_p(0)}. \qquad (2.23)$$

This method essentially enables us to investigate the nature of the inhomogeneity in a nondestructive manner.

C. Exactly solvable model

We shall now illustrate the above properties of localized waves by considering the example of a model that admits of an exact solution. Thus, suppose that $\mu = 0$, the function $f(\psi)$ (see Fig. 2) is piecewise-linear, and all the remaining parameters in (1.1) are independent of time. Equation (1.1) then assumes the following dimensionless form:

$$\dot{\psi} = \psi'' - \psi + p(x, \beta)\,\theta\,[\psi - \psi_1(x, \beta)], \qquad (2.24)$$

where $\theta(x)$ is a step function, [$\theta(x) = 1$ for $x \geqslant 0$ and $\theta(x) = 0$ for $x < 0$], and the point and prime represent differentiation with respect to dimensionless time and the coordinate, respectively. The inhomogeneity is represented by introducing the explicit dependence of $p(x)$ and $\psi_1(x)$ on x. The solution of (2.24) can be found for any $p(x,\beta)$ and $\psi_1(x,\beta)$.

This model is very popular for the description of nonlinear waves in homogeneous systems and, in particular, thermal domains in superconducting microbridges (hot-spot model),[20,79] thin superconducting films,[19] waves that appear in the course of chemical chain reactions on the surface of a solid catalyst,[51,52] waves in gas discharges,[48] and so on. An analysis of the solutions of (2.24) is given in Refs. 80–82 for p = const and ψ_1 = const.

Let us now consider a "strong field" domain localized on a symmetric inhomogeneity ($p(x) = p(-x)$, $\psi_1(x) = \psi_1(-x)$). For the length $2D$ of the portion of the domain in which $\psi > \psi_1$, we then have[24]

$$2\psi_1(D) = e^{-D} \int_{-D}^{D} p(x)\,\mathrm{ch}\,x\,\mathrm{d}x. \qquad (2.25)$$

For a point inhomogeneity, $p(x)$ can be written in the form $p(x) = (1 + \Gamma\delta(x))\,p_0$ and ψ_1 = const. We then have

$$D_{1,2} = \ln \frac{\Gamma \mp \sqrt{\Gamma^2 - 4\xi}}{2\xi}, \qquad (2.26)$$

$$\xi = \frac{2\psi_1(\beta)}{p_0(\beta)} - 1. \qquad (2.27)$$

The quantity β_p for this model is determined by the equation

$$\xi(\beta_p) = 0. \qquad (2.28)$$

As an example, consider a medium heated by a current, in which a phase transition from a highly conducting to a poorly conducting state occurs[22,23] at $T = T_c$ (see Fig. 4a). We then have $\psi_1 = 1$, $\psi = (T - T_0)/(T_c - T_0)$, β is the current density, and α is a parameter determining the Joule heating $p = \alpha\beta^2$ for $\psi > \psi_1$ (for simplicity, we have neglected heat release in the highly-conducting phase with $\psi < 1$). When T_c is independent of β, we find from (2.27) and (2.28) that

$$\xi(\beta) = \left(\frac{\beta_p}{\beta}\right)^2 - 1, \quad \beta_p = \sqrt{\frac{2}{\alpha}}. \qquad (2.29)$$

The function $D(\beta)$ given by (2.26) and (2.29) is shown in Fig. 11, where curve 1 refers to $\Gamma = 0$, curves 2 and 3 refer to $\Gamma > 0$, and curve 4 to $\Gamma < 0$. We recall that, in this example, the quanity Γ determines the additional heat release ($\Gamma > 0$) or heat removal ($\Gamma < 0$) on an inhomogeneity in the poorly-conducting state. The parameters β_r, β_k and D_∞ (see Fig. 11) are, respectively, given by

$$\beta_r = \left(1 + \frac{\Gamma^2}{4}\right)^{-1/2} \beta_p, \quad \beta_k = \beta_p \Gamma^{-1/2},$$

$$D_\infty = \ln\left[\left(1 + \frac{\Gamma^2}{4}\right)^{1/2} - \frac{\Gamma}{2}\right]. \qquad (2.30)$$

It is clear from Fig. 11 that, when $\Gamma < 0$, the inhomogeneity has little effect on the localized "strong field" domain (to the extent that $|\Gamma| \ll 1$). This is illustrated by curves 1 and 4 in Fig. 11. This type of domain exists for $\beta > \beta_p$ (it is represented by point 2 in Fig. 5), which is in agreement with the qualitative analysis given above. The domain represented in Fig. 5 by point 1 is absent from this model because of the presence of the θ-function in (2.24), which ensures that $F \equiv 0$ for $\psi < \psi_1$.

There is a qualitative change in the nature of the solutions describing the "strong field" domains for $\Gamma > 0$. New types of domain (as compared with the homogeneous case)

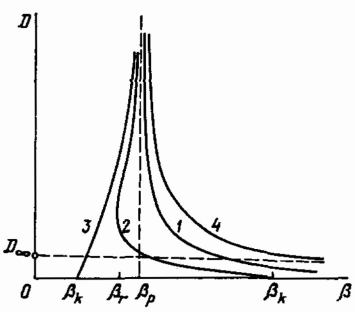

FIG. 11. The function $D = D(\beta)$ for a domain localized on a point inhomogeneity [see (2.26)]: 1—$\Gamma = 0$, 2—$0 < \Gamma < 2$, 3—$\Gamma > 2$, 4—$\Gamma < 0$.

appear with an ascending function $D = D(\beta)$ (see curves 2 and 3 in Fig. 11). Thus, when $0 < \Gamma < 2$, the function $D(\beta)$ has two branches for $\beta_r < \beta < \beta_p$, which correspond to points 2 and 3 in Fig. 5. As $\beta \to \beta_r$, the two domain solutions coalesce into one, and the latter disappears abruptly at $\beta = \beta_r$, where $D(\beta_r) = \ln(2/\Gamma)$. From (2.30), we find that, if $\Gamma \ll 1$, then $\delta\beta = \beta_p \Gamma^2/2$, in complete agreement with the estimate given by (2.14).

The case $\Gamma > 2$ corresponds to strong coupling between the domain and the inhomogeneity. It is clear from Fig. 11 that the properties of the localized domain are then radically different from those of the domain in the homogeneous medium: it exists only for $\beta < \beta_p$ and is characterized by an ascending function $D(\beta)$ in its entire range of existence.

We shall now examine the localization of the domain wall on a point inhomogeneity. In the model that we are currently considering, the condition $\psi(0) > \psi_1$ is obviously satisfied. Consequently, there is a segment of length L_0 to the right of the inhomogeneity on which $\psi > \psi_1$. The static solution of the piecewise-linear equation (2.24) can be obtained in a general form, and hence L_0 can be determined from the equation

$$2\psi_1(L_0) = \int_0^\infty p(x - L_0)\, e^{-x}\, dx. \qquad (2.31)$$

Following the procedure used earlier in this section, let us consider the case of a point inhomogeneity with $p(x) = (1 + \Gamma\delta(x))p_0$, $\psi_1 = \text{const}$. Using (2.31), we then have

$$L_0 = \ln\left(\frac{\Gamma}{\xi}\right). \qquad (2.32)$$

It is clear from (2.32) that the localized domain wall exists only when Γ and ξ have the same sign ($\Gamma > 0$, $\beta < \beta_p$ and $\Gamma < 0$, $\beta > \beta_p$). The expression given by (2.32) is also valid for a point inhomogeneity of a more general type for which

$$f(\psi) = \psi - p_0\theta(\psi - \psi_1) - \Gamma\delta(x). \qquad (2.33)$$

The condition for the domain wall to detach itself from the inhomogeneity is shown by (2.32) to be

$$|\xi| > |\Gamma|. \qquad (2.34)$$

The inequality given by (2.34) will also determine the magnitude of β_2. When $\xi(\beta)$ is given by (2.29), we have

$$\beta_2 = (1 + \Gamma)^{-1/2}\beta_p. \qquad (2.35)$$

When Γ is small, we have from (2.35) $\beta_p - \beta_2 \approx \Gamma\beta_p/2$, which is in agreement with the estimate given above. When the domain wall is strongly coupled to the inhomogeneity ($|\Gamma| \sim 1$), we can readily show, by comparing (2.35), (2.29), and (2.34), that the domain wall can become localized for $|\Gamma| \gg 1$ in the entire range of existence of the two-phase state.

When a smooth inhomogeneity ($\varepsilon \ll 1$) is present, the quantities $p(x)$ and $\psi_1(x)$ in (2.24) are slowly-varying functions on a scale of ~ 1. Let us suppose, for simplicity, that $p(x) = (1 - sx^2)p_0$, where $s \sim \varepsilon^2 \ll 1$, so that we obtain the following result from (2.25):

$$\exp(-2D) + sD^2 + \xi(\beta) = 0. \qquad (2.36)$$

When $0 < s \ll 1$, this equation has two roots with essentially different D: $D_1 \approx 0.5\ln(1/|\xi|)$, $D_2 \approx s^{-1/2}\sqrt{|\xi|}$. The two branches of the function $D = D(\beta)$ coalesce for $\beta = \beta_r \approx \beta_p(0) + O(\varepsilon^2 \ln^2(1/\varepsilon))$, where, for $\beta \simeq \beta_r$

$$D(\beta) = D_c \pm M\sqrt{\beta - \beta_r}, \qquad (2.37)$$

and $D_c \equiv D(\beta_r) \approx 0.5\ln(1/s)$, $M = \sqrt{|\partial\xi/\partial\beta|/2sD_c}$, $\partial\xi/\partial\beta < 0$ [see, for example, (2.29)]. Thus, when $\varepsilon \ll 1$, the function $D = D(\beta)$ is similar to curve 2 in Fig. 11 as $\beta_k \to \infty$ and $\beta_p \to \beta_p(0)$.

D. Dynamics of localized waves

All the waves localized on inhomogeneities in which we are interested here are essentially nonlinear, so that their stability against finite-amplitude perturbations becomes an important question, and so is the dynamics of the localization of a propagating wave on an inhomogeneity. In the situations examined here, the homogeneous state is stable to small perturbations. Consequently, the waves examined above will appear only in response to finite-amplitude perturbations (hard wave excitation regime[83]). The solution of such problems requires the investigation of nonself-preserving solutions of (1.1), which is not possible in the general case. On the other hand, the basic qualitative aspects of the dynamics of localized waves can be elucidated even by analyzing the simple model discussed in the last section.

Suppose that, for $t = 0$, an external influence produces a region in the neighborhood of a point inhomogeneity with $p(x) = [1 + \Gamma\delta(x)]p_0$ [see (2.24)], in which $\psi > \psi_1$. The length of this region is $D(0) = D_+(0) + D_-(0)$, where $D_+(t)$ and $D_-(t)$ are the distances from the inhomogeneity to the right- and left-hand boundaries of this region, respectively (see Fig. 12).

Consider the dynamics of this initial perturbation, restricting our attention to the case where $|\Gamma| \ll 1$. The domain can then be localized on the inhomogeneity in a narrow interval $\delta\beta$ near β_p, in which its equilibrium length is $D \gg 1$ [see (2.26)–(2.29)] and the velocity of the domain wall is small $v \sim \delta\beta/\beta_p \ll 1$ [see (2.25)]. If the initial distribution $\psi = \psi_0(x)$ is such that the length of the domain is much greater than the width of its boundaries (Fig. 12), its subsequent evolution in time can be divided into two stages. In a time ~ 1 during the first stage, the distribution $\psi_0(x)$ relaxes to the quasiequilibrium distribution in the range $-D_-(0) \lesssim x \lesssim D_+(0)$ in which $\psi = \psi_2$.[3)] The length of this region begins to vary slowly with time during the second stage. The rate of this variation is determined by the velocities of the domain walls, which are small for $\beta \simeq \beta_p$. The characteristic time for a change in $D_\pm(t)$ is of the order of $D_\pm/v \gg 1$. This enables us to reduce the relatively complicated nonlinear integral equation for $\psi(x,t)$ to a set of two ordinary differential equations[84] for $D_\pm(t)$:

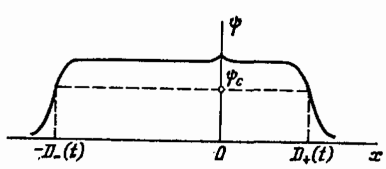

FIG. 12. The distribution $\psi = \psi(x,t)$ during the localization of a domain.

[3)]The dimensions $D_\pm(t)$ change by ~ 1 during this time.

$$\frac{1}{2}\dot{D}_{\pm} + \frac{\dot{p}}{p} = -\xi(\beta) + \Gamma e^{-D_{\pm}} - e^{-(D_{\pm}+D_{\mp})}. \qquad (2.38)$$

The appearance of the term $\dot{p}/p$ in (2.38) is connected with the possible time dependence of the parameter β. It is clear from (2.38) that the slow variation in $D_{\pm}(t)$ is determined by the smallness of the quantities ξ, Γ, $\dot{p}/p$ and $\exp[-(D_+ + D_-)]$.

Let us now begin by considering the stability of the localized waves against small perturbations. Assuming that $D_{\pm}(t) = D + \delta D_{\pm} \exp\lambda t$, $D \gg \delta D_{\pm}$, we find that the growth rate of the most "dangerous" perturbations $(\delta D_+ = -\delta D_-)$ is

$$\lambda = 2(2e^{-D} - \Gamma)e^{-D}, \qquad (2.39)$$

where D is given by (2.26). When $\Gamma < 0$, we have $\lambda > 0$, i.e., the localized "strong field" domain is always unstable. On the other hand, when $\Gamma > 0$, the function $\lambda(\beta)$ vanishes for $D = D_c = \ln(2/\Gamma)$, where $\lambda > 0$ for $D < D_c$ and $\lambda < 0$ for $D > D_c$. Comparison of (2.26) and (2.30) shows that $\lambda = 0$ for $\beta = \beta_r$ and $\xi(\beta_r) = \Gamma^2/4$. Thus, the entire ascending branch of the function $D(\beta)$ in Fig. 11 is stable, and the descending branch is unstable.

It has been assumed throughout the foregoing discussion that $\beta = \text{const}$. It is, however, possible to have a situation where the parameter β is a function of $2D(t) = D_+ + D_-$ because of the presence of a measure of feedback in the system. This feedback may stabilize the domains that are unstable for $\beta = \text{const}$.

As a simple example, consider the case where β is the transport current flowing through a specimen connected to a load of resistance r and inductance $\mathscr{L}$. For the sake of simplicity, we shall suppose that the entire electrical potential difference develops across the domain alone (this occurs, for example, in superconductors[19–21]), so that

$$\mathscr{L}\dot{\beta} + (r + 2D)\beta = r\beta_0, \qquad (2.40)$$

where the quantities $\mathscr{L}$, r, and D have been made dimensionless by dividing them by quantities that are characteristic for each specific problem. Linearizing (2.38) and (2.40), it can be shown that the domain that was stable for $\beta = \text{const}$ [ascending branch of the function $D = D(\beta)$ in Fig. 11] remains stable in the present case as well. On the other hand, the domain that was unstable for $\beta = \text{const}$ [descending branch of $D = D(\beta)$ in Fig. 11] is stabilized by the feedback loop if $\mathscr{L} < \mathscr{L}_k$, where

$$\mathscr{L}_k = \left[\frac{1}{2}(r + 2D) - 4\right] e^{2D}(2 - \Gamma e^{D})^{-1}; \qquad (2.41)$$

in which $D(\beta) \gg 1$ is given by (2.26). We note that, as $\beta \to \beta_r$, we have $\mathscr{L}_k \to \infty$. The self-oscillatory state with frequency $\omega \sim \mathscr{L}^{-1}$ sets in for $\mathscr{L} > \mathscr{L}_k$. Such self-oscillations can occur in a great variety of systems, including superconducting films,[20,85,86] ultrathin superconducting threads,[87] composite semiconductors,[88,89] semiconducting structures,[90,91] and so on.

Let us now examine the stability of a localized domain wall (Fig. 7). From (2.39), we now have

$$\lambda = -2\Gamma \exp(-L_0). \qquad (2.42)$$

Thus, in the model defined by (2.42), the localized wall is stable only for $\Gamma > 0$. The absence of stable ($\lambda < 0$) solutions

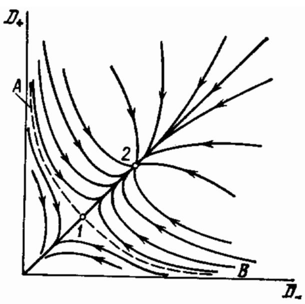

FIG 13. Phase portrait of the system (2.38) for $0 < \xi < \Gamma^2/4$ and $\Gamma > 0$.

for $\Gamma < 0$ is connected with the fact that, in this model, $F(\psi) \equiv 0$ for $\psi < \psi_1$. If, on the other hand, $f(\psi)$ is given by (2.33), the localization of the stable domain wall is possible in the range $0 < |\xi| < |\Gamma|$ for any sign of Γ.

We now turn to the stability of a localized "strong field" domain against finite-amplitude perturbations. The phase portrait[83] of (2.38) for $\beta = \text{const}$ is shown in Fig. 13 for $0 < \xi < \Gamma^2/4$. The two possible states of the domain on the inhomogeneity ($\Gamma > 0$) correspond to the two singular points 1 and 2, where 1 (saddle) corresponds to the unstable and 2 (node) to the stable state of the domain. The domain dynamics depends on the position of its phase trajectory on Fig. 13. If the mapping point corresponding to the initial ($t = 0$) state of the domain $[D_+(0), D_-(0)]$ lies to the right of the separatrix AIB (broken line in Fig. 13), then, as $t \to \infty$, the domain becomes trapped by the inhomogeneity. In the opposite case, the domain collapses before it succeeds in localization.

The domain localization dynamics can be divided qualitatively into two stages. During the first stage, there is a relatively rapid independent motion of the domain boundaries, which leads to its symmetrization ($D_+ \approx D_-$). This is followed by either a slow [see (2.39)] relaxation of the domain to its stable state on the inhomogeneity ($\dot{D}_+ > 0$ for $D_1 < D_+ < D_2$ and $\dot{D}_+ < 0$ for $D_+ > D_2$), or the domain vanishes altogether for $D_+ < D_1$.

To conclude this section, let us consider the localization dynamics of a domain wall on a point inhomogeneity. If, for example, the wall (see Fig. 7) moves from right to left ($\Gamma > 0$, $\xi > 0$), we must substitute $D_- \to \infty$, $D_+(t) \equiv L_0(t)$ in (2.38) and obtain

$$L_0(t) = \ln\left[\frac{\Gamma}{\xi} + \left(e^{L_0(0)} - \frac{\Gamma}{\xi}\right)e^{-2\xi t}\right] \qquad (2.43)$$

from which it is clear that, for $L_0(0) \gg L_0(\infty) = \ln(\Gamma/\xi)$, the domain wall moves uniformly ($L_0(t) = L_0 - 2\xi t$) and, as it approaches the inhomogeneity ($L_0 \sim L_0(\infty)$), its velocity falls off exponentially.

The model that we are discussing will also lead us to the equation describing the slow domain-wall dynamics in a medium containing several inhomogeneities, in which case $f(\psi) = \psi - p_0\theta(\psi - \psi_1) + \Sigma_i \Gamma_i \delta(x - x_i)$, where $\Gamma_i = \text{const}$. Using the results reported in Ref. 84, we find that

$$\frac{1}{2}\dot{L}_0 = -\xi(\beta) + \sum_i \Gamma_i \exp(-|x_i - L_0|), \qquad (2.44)$$

where $\xi(\beta)$ corresponds to the homogeneous part of the specimen.

3. LOCALIZED STATIC WAVES (GENERAL APPROACH)

In this section, we shall summarize the formulas that enable us to describe the general case, where the parameters in (1.1) are arbitrary functions of time. We shall be interested in static solutions of this equation that describe localized waves, the conditions for their existence, and their stability. Such questions have been examined in several papers (see, for example, Refs. 11, 15, 18, 22–24, and 29) in relation to different physical systems. In our presentation, we shall essentially follow Refs. 23 and 24.

A. Static distributions

Let us begin by considering the "strong field" domain localized on a point inhomogeneity ($\varepsilon \gg 1$). The distribution $\psi(x)$ outside the inhomogeneity is obtained by direct integration of (1.1) with $\dot{\psi} = 0$. In the interior of the inhomogeneity, $\psi(x)$ varies little for $\varepsilon \gg 1$, which enables us to find $\psi(x)$ by substituting $\psi = \psi_m$ in the functions $f(\psi,x)$ and $\varkappa(\psi,x)$ in (1.1). By joining the solutions obtained in this way on the inhomogeneity boundaries, we obtain the distribution $\psi = \psi(x)$ in the domain:

$$|x(\psi)| = 2^{-1/2} \int_{\psi}^{\psi_m} \varkappa S^{-1/2}\, d\psi, \tag{3.1}$$

where the functions $\varkappa(\psi)$ and $S(\psi)$ [see (2.2)] are determined by the homogeneous part of the specimen and ψ_m is a root of (2.10) where[23]

$$F^2(\psi_m) = \left[\int_{-l}^{l} f(\psi_m, x)\, dx\right]^2 - 8\varkappa_m f_m \int_0^l \frac{dx}{\varkappa(\psi_m, x)} \int_0^x f(\psi_m, x')\, dx', \tag{3.2}$$

in which f_m and $\varkappa_m$ are the values of f and $\varkappa$ outside the inhomogeneity for $\psi = \psi_m$. In an inhomogeneous medium in which f and $\varkappa$ are not explicit functions of x, we have $F \equiv 0$. Equation (2.10) together with the expression for $F(\psi)$ given by (3.2) enable us to examine all the possible types of domains that can be localized on a point inhomogeneity of arbitrary physical nature. It is important to note here that, because of the essential dependence of F on ψ, the inhomogeneity then plays the role of a self-consistent point source whose strength depends on the distribution $\psi = \psi(x)$ in the domain.

The critical values β_r and β_k, for which new types of localized domain appear (see Figs. 5 and 11) are determined from (2.13), where $T \equiv \psi$, $T_m \equiv \psi_m$ and $F = F(\psi)$ is given by (3.2).

The solutions describing the domain wall localized on an inhomogeneity can be constructed in an analogous manner. Assuming, to be specific, that $\psi(-\infty) = \psi_2$, $\psi(\infty) = \psi_0$, $F > 0$, $\beta < \beta_3$ (see Fig. 7), we obtain

$$x(\psi) = 2^{-1/2} \int_{\psi}^{\psi_m} \varkappa S^{-1/2}\, d\psi, \quad x > 0, \tag{3.3}$$

$$x(\psi) = -2^{-1/2} \int_{\psi_m}^{\psi} \varkappa (S - S_2)^{-1/2}\, d\psi, \quad x < 0. \tag{3.4}$$

The quantity $\psi_m \equiv \psi(0)$ in (3.3) and (3.4) is determined, as before, from the condition for joining the solutions inside and outside the inhomogeneity:

$$S(\psi_m) = \frac{F^2(\psi_m)}{8} + S_2 + \frac{S_2^2}{2F_1^2(\psi_m)} \equiv R(\psi_m), \tag{3.5}$$

$$F_1(\psi_m) = \int_{-l}^{l} \left[f(\psi_m, x) - \frac{f_m \varkappa_m}{\varkappa(\psi_m, x)}\right] dx. \tag{3.6}$$

Comparison of (3.5) and (3.6) with (2.17), where the latter is obtained on the assumption of a point inhomogeneity, shows that they are identical only for $F = F_1$, i.e., when the inhomogeneity produces a strong change in $f(\psi,x)$ and a weak change in $\varkappa(\psi,x)$, and the second term in (3.2) and (3.6) can be neglected.

The necessary condition for the existence of localized domain walls is the existence of nontrivial solutions of (3.5) and (3.6). The critical value β_2 for which such solutions disappear can be determined from the following system that is analogous to (2.13):

$$S(\psi_m, \beta_2) = R(\psi_m, \beta_2), \quad \frac{\partial}{\partial \psi_m}[S(\psi_m, \beta_2) - R(\psi_m, \beta_2)] = 0. \tag{3.7}$$

Let us now consider the opposite case of a smooth inhomogeneity[24,29] ($\varepsilon \ll 1$). When $D \sim L$ (see Fig. 1a), the coefficients of (1.1) that depend explicitly on x can be expanded into a series in x, and we retain only terms $\propto x^2$. The variable x can then be expressed in terms of ψ in these expansions, if we use the implicit relationship $x = x_0(\psi)$ for the domain in the homogeneous medium with parameters $f = f_0(\psi) \equiv f(\psi,0)$ and $\varkappa = \varkappa_0(\psi) \equiv \varkappa(\psi,0)$. The final result is

$$|x| = 2^{-1/2} \int_{\psi}^{\psi_m} \left[\varkappa_0 + \frac{x_0^2}{2} \frac{\partial^2 \varkappa}{\partial x^2}\Big|_0\right] \tilde{S}^{-1/2}\, d\psi, \tag{3.8}$$

$$\tilde{S}(\psi) = \int_{\psi_0}^{\psi} \left[\varkappa_0 f_0 + \frac{x_0^2}{2} \frac{\partial^2}{\partial x^2}(\varkappa f)\big|_0\right] d\psi, \tag{3.9}$$

where

$$|x_0(\psi, \psi_m)| = 2^{-1/2} \int_{\psi}^{\psi_m} \varkappa_0 S_0^{-1/2}\, d\psi, \tag{3.10}$$

$$S_0(\psi) = \int_{\psi_m}^{\psi} \varkappa_0 f_0\, d\psi \tag{3.11}$$

[for simplicity, it was assumed in the derivation of (3.8)–(3.11) that the inhomogeneity was symmetric]. The equation for ψ_m in (3.8)–(3.11) has the form

$$\tilde{S}(\psi_m) = 0. \tag{3.12}$$

This method of solving the nonlinear equation (1.1) enables us to describe the appearance of a new branch of solutions for $\beta \gtrsim \beta_r$, which are absent in the homogeneous medium (Ref. 24).[4)]

The equations from which β_r can be determined are analogous to (2.4):

$$\tilde{S}(\psi_m, \beta_r) = 0, \quad \frac{\partial}{\partial \psi_m} \tilde{S}(\psi_m, \beta_r) = 0. \tag{3.13}$$

[4)]This approach is equivalent to the Rauscher method, well known in the theory of nonlinear oscillations (see, for example, Ref. 92).

When β is only just greater than β_r ($\delta\beta \sim (\varepsilon \ln(1/\varepsilon))^2\beta_r$), the size of the domain corresponding to the ascending branch of the function $D(\beta)$ becomes much greater than D_c. When $D \gg D_c$, the quantity D is determined from (2.22), and the distribution $\psi = \psi(x)$ in the domain can be found on the basis of the following considerations.[24,29]

To within terms $\sim\varepsilon$, the stationary state of the phase with $\psi = \psi_2$ in the domain with $D \gg L$ is determined from the local balance condition $f(\psi,x) = 0$ everywhere with the exception of the domain boundaries ($|x| \approx D_\pm$), where $\psi(x)$ changes from $\psi \approx \psi_2$ to $\psi \approx \psi_0$ over a length $\sim L$. The function $\psi = \psi(x)$ can be found on the domain walls by expanding $f(\psi,x)$ and $\varkappa(\psi,x)$ into a series in powers of $(|x| - D_\pm)$. If we then join the solutions for the exterior ($|x| \lesssim D_\pm$) and interior ($|x| \gtrsim D_\pm$) regions of the domain, we find that the self-consistent equation $D_\pm = D_\pm(\beta)$ becomes identical with (2.22) to zero order in ε (a more rigorous development of domain solutions for $\varepsilon \ll 1$ is given in Ref. 29, using the method of singular perturbations[93]).

B. Stability of localized waves

Let us now consider the stability of waves localized on an inhomogeneity against small perturbations $\delta\psi(x,t)$:

$$\delta\psi(x,t) = \varkappa^{-1} \sum_{n=0}^{\infty} y_n(x) e^{\lambda_n t}, \tag{3.14}$$

where λ_n are the eigenvalues and $y_n(x)$ are the eigenfunctions to be determined. When $\varepsilon \gg 1$, the equation for $y_n(x)$ is

$$y_n'' - \left[\gamma_n + \frac{1}{\varkappa}\frac{df}{d\varphi} - \frac{1}{\varkappa}\frac{dF}{d\psi}\delta(x)\right] y_n = 0, \tag{3.15}$$

where the prime represents differentiation with respect to x, $\gamma_n = \varkappa^{-1}\lambda_n(\nu + \mu\lambda_n)$, and the coordinate dependence of μ, ν, $\varkappa$, F and f is determined by their dependence on the stationary solution $\psi(x)$. Clearly, the wave is unstable if there is at least one eigenvalue $\lambda_n > 0$. We shall be interested in the quantity $\lambda_0 = \max \lambda_n$, $n = 0, 1, 2, \ldots$, that determines the stability boundary $\lambda_0 = 0$.

We shall seek the solution of (3.15) in the form $y(x) = z(x)\cdot\exp(\int u\,dx)$, where $z(x) = \varkappa\psi'(x)$. We then obtain for $u(x)$ the following first-order equation:

$$u' + 2\frac{z'}{z}u + u^2 = \gamma. \tag{3.16}$$

The quantity λ_0 is small near the stability boundary, and the function $u = u(x)$ can be sought in the form of a series in λ_0. This leads to the following equation for λ_0 (see, for example, Ref. 23):

$$\lambda_0 = (-1 \pm \sqrt{1 + 4k\lambda_c})\frac{1}{2k} \tag{3.17}$$

$$k = \int_{\psi_0}^{\psi_m} \mu\sqrt{S}\,d\psi \Big/ \int_{\psi_0}^{\psi_m} \nu\sqrt{S}\,d\psi,$$

$$\lambda_c = \frac{F}{2^{3/2}\varkappa \int_{\psi_0}^{\psi_m} \nu\sqrt{S}\,d\psi} \frac{d}{d\psi_m}\left(\frac{F^2}{8} - S\right). \tag{3.18}$$

The localized "strong field" domain is stable if $\lambda_c < 0$, and this leads to the condition given by (2.12) that was obtained above from qualitative considerations (in the neighborhood of the bifurcation points β_r and β_k). Strictly speaking, the expressions given by (3.17) and (3.18) are valid only for $\lambda_0 \to 0$, $\lambda_c \to 0$ (see Ref. 23), so that the square root in (3.17) can be expanded into a series, except when the quantity k is anomalously high. The latter occurs, for example, in a Josephson contact,[13] where the damping of perturbations is oscillatory in character, even near the stability threshold ($4k\lambda_c < -1$).

Similarly, as $\lambda_0 \to 0$, we obtain the following expression for the localized domain wall:

$$z^{-2}(+0)\int_0^\infty \gamma_0 z^2\,dx + z^{-2}(-0)\int_{-\infty}^0 \gamma_0 z^2\,dx$$
$$= \frac{d}{d\psi}[F + z(+0) - z(-0)]_{\psi_m}; \tag{3.19}$$

where the expression for $z(x) = \varkappa\psi'(x)$ follows from (3.3) and (3.4). The stability condition $\lambda_0 < 0$ ($\gamma_0 < 0$) leads to the condition given by (2.18) and obtained above for the neighborhood of the bifurcation point $\beta = \beta_2$ on the basis of qualitative considerations. Thus, the delocalization of the domain wall at $\beta = \beta_2$ is connected with the loss of stability. We note, however, that, in the model defined by (2.24), the quantity λ remains finite at $\beta = \beta_2$ [see Eq. (2.42)]. This is connected with the nonanalytic behavior of the function $S(\psi)$ at $\psi = \psi_1$.[5)]

Let us now examine in greater detail the situation prevailing in the neighborhood of the bifurcation point $\beta = \beta_3$, where $2|S_2| = F^2$. The right-hand side of (3.19) vanishes for $\beta = \beta_3$ but, simultaneously, the coefficient γ_0 on the left-hand side of (3.19) becomes infinite. This is so because the "momenta" $z(\pm 0)$ vanish for "trajectories" corresponding to points 3 and 2. The fact that the coefficient of γ_0 becomes infinite indicates that perturbation theory developed for the derivation of (3.19) is invalid and, consequently, the relation given by (3.19) itself is invalid in the neighborhood of $\beta = \beta_3$. Thus, the stability criterion given by (2.18) is invalid at the bifurcation point $\beta = \beta_3$. As already noted, physically, this is connected with the finite growth rate of perturbations at $\beta = \beta_3$.

Analysis of the stability of the localized domain for $\varepsilon \ll 1$ shows[24] that, when $D \gg D_c \sim L\ln(1/\varepsilon)$, the expression for λ_0 ($\mu = 0$) is identical with the formula given by (2.21) and obtained on the basis of quantitative considerations. If, on the other hand, $D < D_c$, then λ_0 changes sign, and this corresponds to the instability of the descending branch of the function $D(\beta)$ (see Fig. 11, curve 2).

4. EXAMPLES

In this section, we shall examine a number of special cases that can be described with the aid of (1.1). We shall be interested only in phenomena connected with the presence of inhomogeneities, so that the list of references referring to this part of our review will undoubtedly be incomplete.

[5)]The discontinuous reconstitution of stable structures, described by two coupled nonlinear parabolic equations, is examined in Ref. 94.,

A. Resistive domains in superconductors

Under the influence of external fields, a superconductor can assume different inhomogeneous states that can be either in thermodynamic equilibrium (intermediate state and vortex structure in superconductors of the first and second type[95,96]) or well away from thermodynamic equilibrium. The latter will be considered later.

There is a great variety of methods for producing nonequilibrium inhomogeneous states, including effects due to transport currents,[19–24,27,28] laser and microwave radiation,[97,100] ultrasound,[101–102] tunnel electron injection,[103–107] and so on.

To provide a quantitative description of nonequilibrium states in superconductors, one must turn to the dynamic equations of the theory of superconductivity.[62,108–110] There are, however, many cases for which these relatively complex equations can be reduced to a single equation analogous to (1.1). Depending on the particular conditions (see, for example, Refs. 62 and 108–110), this equation will describe the diffusion of electronic excitation, the distribution of the order parameter, temperature distribution, and so on.

Here, we shall consider the situation where only thermal effects are important. In superconductors in which a transport current I is flowing, we have, in the simplest case,

$$Q = j^2\rho(j, T) \times \begin{cases} 0, & T < T_c(j), \\ 1 - j_c/j, & T > T_c(j), \end{cases} \qquad (4.1)$$

where j is the current density, ρ is the resistivity in the resistive state, j_c is the critical current density due to either the pinning of the vortex lattice in type II superconductors[111] or the critical velocity of the superconducting condensate in thin films.[112]

Figure 4a[6)] shows the functions $Q(T)$ and $W(T)$ for superconductors carrying a current $[Q(T) = 0$ for $T < T_c]$. Consequently, such semiconductors may contain resistive domains, i.e., regions of finite size in the normal (resistive) state due to Joule heating.[19–21] They are, at the same time, electric-field domains.

Let us consider the localization of resistive domains on point inhomogeneities due to, for example, reduced values of j_c and ρ, which may be connected with a reduction in the height of the surface barrier to the entry of vortices,[27,113] a change in the transverse cross section of the specimen, the presence of grain boundaries or inclusions of a different phase (especially in granulated films), and so on. In most cases, such inhomogeneities obviously act as "nuclei" for the formation of resistive domains upon them.

All the features connected with the localization of resistive domains are particularly clearly defined on the current-voltage characteristics $V = V(j)$ of a superconductor, where

$$V(j) = \sqrt{2} \int_{T_c}^{T_m} \varkappa\rho(j - j_c)\, S^{-1/2}\, dT + jA\Delta R \qquad (4.2)$$

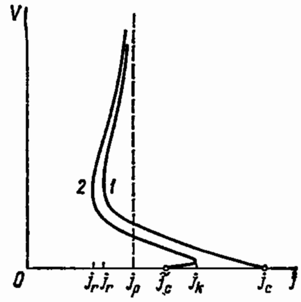

FIG. 14. Current-voltage characteristic of a superconductor with a localized resistive domain in the presence of an inhomogeneity in the resistivity alone (curve 1) and in both critical current and resistivity curve (2) (the bars on the j axis to the right of 0 correspond to $j_2^2\, j_2^1$).

in which $V(j)$ is the potential difference across the superconductor containing the domain, T_m is a root of Eqs. (2.10) and (3.2), in which $\beta \equiv j$, $\psi_m \equiv T_m$, ΔR is the excess resistance of the inhomogeneity, and A is the cross-sectional area of the specimen. The current-voltage characteristic is then multivalued and (4.2) describes the branch of the characteristic that corresponds to this domain solution.

Figure 14 shows typical current-voltage characteristics of a superconductor with a resistive domain localized within it. Curve 1 corresponds to an inhomogeneity in $\rho = \rho(x)$ alone, which is an additional source of heat in the resistive state, and curve 2 corresponds to an inhomogeneity in both[22,23] $\rho(x)$ and $j_c(x)$. In Fig. 14, j_c is the critical current density, $\tilde{j}_c$ is the critical current density on the inhomogeneity, j_r and j_k are current densities determined from (2.13) with $\beta_{r,k} \equiv j_{r,k}$, and j_p is determined from (2.4) with $\beta_p \equiv j_p$. The quantity I_p is called the minimum current for the propagation of the normal phase[37,38] and can be estimated by equating the Joule heat release ρj_p^2 in the resistive $(T > T_c)$ phase to the heat removed by the coolant $h(T - T_0)/d$. On the $T_c - T_0$ temperature scale that is characteristic for a superconductor, this gives

$$j_p \sim \left(\frac{dT_c}{\rho h}\right)^{1/2} \left(1 - \frac{T_0}{T_c}\right)^{1/2}. \qquad (4.3)$$

Phenomena connected with Joule heating in superconductors will obviously become important for $j_p \lesssim j < j_c$. For films, for example,[112] $j_c \approx j_0[1 - (T/T_c)]^{3/2}$, so that, as $T \to T_c$, we have $j_c \ll j_p$, i.e., thermal phenomena can be neglected in the temperature range $T_c - T_0 \lesssim T_c\, j_0^{-1}\sqrt{hT_c/\rho d}$.

For the current densities j_r and j_k of Fig. 14, we have the order of magnitude estimates $j_c - j_k \sim \Gamma j_c$, $j_p - j_r \sim \Gamma^2 j_p$, where $\Gamma \sim \Delta\rho l/\rho L$, and $\Delta\rho$ is the change in $\rho = \rho(x)$ in the interior of the inhomogeneity.

Many-valuedness and the presence of descending branches on the current-voltage characteristics (Fig. 14) result in hysteresis in phenomena accompanying the removal (restoration) of superconductivity by a current.[22,23] Bounded, stable, resistive regions that do not extend to the entire specimen can then be present in the superconductor in a broad range of currents $\min(\tilde{j}_c, j_r) < j < j_k$ even in the simplest case.

[6)]There is also the possibility of a larger number of crossing points between $Q(T)$ and $W(T)$ due to, for example, the peak effect in a critical current,[111] the coolant boiling crisis,[37] and so on.

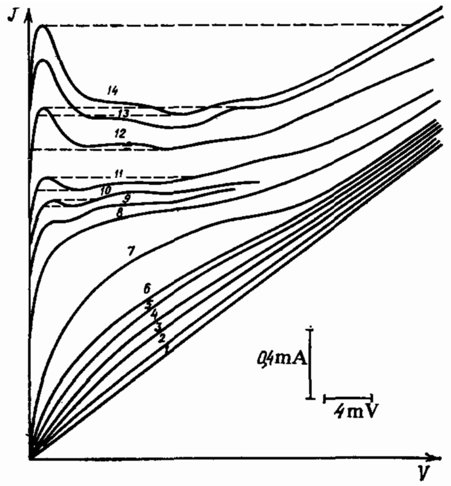

FIG. 15. Current-voltage characteristic of a granulated In film[28] for different values of $\xi_0 = 1 - (T_0/T_c)$: 1—$\varepsilon_0 = 0$, 2—8×10^{-4}, 3—4.7×10^{-3}, 4—6.1×10^{-3}, 5—7.5×10^{-3}, 6—9.1×10^{-3}, 7—1.19×10^{-2}, 8—1.4×10^{-2}, 9—1.46×10^{-2}, 10—1.52×10^{-2}, 11—1.63×10^{-2}, 12—1.79×10^{-2}, 13—1.9×10^{-2}, 14—2.07×10^{-2}.

Current-voltage characteristics similar to those shown in Fig. 14 have frequently been recorded experimentally.[28,88,114,115] In particular, Fig. 15 shows the CVC of a granulated In film obtained experimentally in Ref. 28, where it was also shown that the temperature functions $\rho(T)$ and $\tilde{j}_c(T)$ in the interior of an inhomogeneity may be essentially different from the corresponding functions for the homogeneous part of the film, and this must be taken into account if correct interpretation of experimental data is to be achieved. As $T_0 \rightarrow T_c$, the CVC shown in Fig. 15 is single-valued but, as T_0 is reduced, it becomes multivalued and a descending branch appears (see also Ref. 115). In Figs. 3 and 5, this corresponds to a transition from the region in which $\beta \ll \beta_1 \sim \beta_p$ to the region in which $\beta \sim \beta_p$.

The CVC of a superconductor containing a resistive domain localized on a smooth inhomogeneity ($\varepsilon \ll 1$) is shown in Fig. 14 (curve 1, where $j_r \approx j_p(0)$, $j_p = j_p(\infty)$, $j_c = j_c(0)$) and in Fig. 16. Depending on the parameter values, we can have $j_c(0) > j_p(\infty)$ (see Fig. 14) or $j_c(0) < j_p(\infty)$ (Fig. 16). In the former case, an increase in the current is accompanied by a transition of the specimen to the normal state for which $j = j_c(0)$ and back again, i.e., from the normal state to the superconducting state, beginning with $j = j_p(0) < j_c(0)$. Thus, for current densities in the range $j_p(0) < j < j_p(\infty)$, the specimen is in the resistive state owing to the localization within it of the resistive domain.

FIG. 16. Current-voltage characteristic of a superconductor with a resistive domain localized on a smooth inhomogeneity for $\tilde{I}_c < I_p(\infty)$.

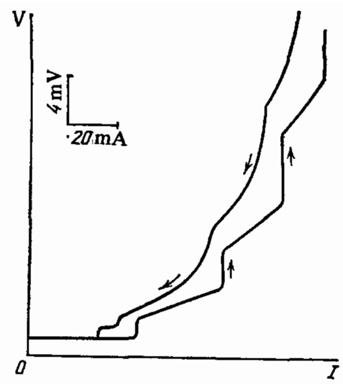

FIG. 17. Current-voltage characteristic of a granulated In film.[27]

When $j_c(0) < j_p(\infty)$ (see Fig. 16), a localized domain appears on the inhomogeneity for $j = j_c(0) > j_p(0)$, but the remainder of the specimen remains superconducting. Hysteresis is observed when the current is reduced, since superconductivity is restored for $j \approx j_p(0) < j_c(0)$. For $j_c(0) < j_p(0)$, the CVC of the specimen containing the resistive domain is similar to curve 3 of Fig. 11 and, clearly, hysteresis is absent.

When the specimen contains several inhomogeneities, the CVC may consist of a number of steps due to the successive appearance of resistive domains within each of the inhomogeneities, as the current increases. Hysteresis occurs as the current j is reduced, because of the difference between $j_c(X_n)$ and $j_p(X_n)$, where X_n is the coordinate of the n-th inhomogeneity $(j_c(X_n) > j_p(X_n))$. The steps on the CVC will also appear if there are just a few inhomogeneities producing a nonmonotonic function $I_p(X)$ (see Fig. 10). The suppression of superconductivity by the current then begins locally on a "weak" point for which $\tilde{j}_c < j$, and subsequently continues in a stepwise manner (see insert in Fig. 10). Figure 17 shows the CVC of a granulated In film, obtained experimentally in Ref. 27, which is in complete agreement with the picture given above.

We note that the hysteresis, the steps, and the breaks on the current-voltage characteristics of thin superconducting films have been reported frequently[27,28,113–117] and can probably be explained by the influence of inhomogeneities. Alternative (nonthermal) mechanisms that may be responsible for steps on the CVC's include, for example, the appearance of phase-slip centers,[118,119] the entry of vortex "strings" into the specimen,[113,120] metastable states of the vortex lattice of macroscopic defects[121,122] and so on. These mechanisms play a major role in the evolution of the resistive state as $T \rightarrow T_c$ but, if the number of vortices or phase-slip centers on the characteristic thermal length L is much greater than unity, a transition to the macroscopic description given above takes place.

B. Optical discharge in gases

Ionization waves that accompany the propagation of a powerful laser beam in a gas (see, for example, Refs. 47 and

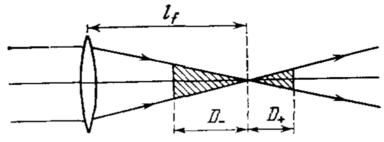

FIG. 18. Plasma domain in an optical gas discharge.

48) are a very interesting example of localized domains. Plasma condensations (domains) that exist because of the heating and ionization of the gas by the incident radiation may be formed in this type of beam. The plasma temperature ($T \sim (1\text{–}3)\cdot 10^4$ K) is determined by the balance between the heat liberated Q and the heat W removed into the ambient cold gas.

Here, we shall confine our attention to the "slow light burn" state.[48] In this case, the laser power is insufficient for the direct ionization of the gas, and the velocity of the boundaries of the plasma region is small in comparison with the velocity of sound. When the gas pressure is not too high, the evolution of the plasma domain can be described in the first approximation by the following set of equations (see, for example, Ref. 48)

$$\nu \frac{\partial T}{\partial t} = \frac{\partial}{\partial x} \varkappa \frac{\partial T}{\partial x} + cP\mu_\omega(T) - \frac{\gamma}{r^2}\varkappa(T - T_0), \qquad (4.4)$$

$$\frac{\partial J}{\partial x} + \mu_\omega(T) J = 0; \qquad (4.5)$$

where x is the coordinate along the beam of radius $r(x)$ (Fig. 18), $P(x)$ is the energy flux density in the incident radiation per unit time, $J(x) = \pi r^2 P$ is the beam power, $\mu_\omega(T)$ is the light absorption coefficient, and γ is a numerical factor of the order of unity. Clearly, Eq. (4.5) describes the attenuation of the laser-beam intensity as a result of the absorption of light.

The absorption coefficient $\mu_\omega(T)$ rises rapidly for $T > T_c$, where T_c is of the order of the gas ionization temperature (see, for example, Refs. 123). Thus, the temperature dependence of the heat release $Q(T) = cP\mu_\omega$ has a characteristic form similar to that shown in Fig. 4a. When the $Q(T)$ and $W(T)$ curves have three crossing points, we have the possibility of a self-sustaining state in which the plasma absorbs light energy incident upon it, and heats up to temperature $T = T_3 > T_c$ (see Fig. 4a). The function $U = U(T)$ is then identical with that shown in Fig. 5, where the role of the parameter β is now played by J, and the region occupied by the plasma is a "strong-field" domain.

Figure 18 shows the scheme of a "slow light burn" experiment.[47] Focusing of the laser beam gives rise to an inhomogeneity of the external conditions in which the gas is situated, and thus to the localization of the plasma domain in the region of the focus (the characteristic scale of the inhomogeneity is obviously of the order of the focal length l_f of the lens). In accordance with the foregoing analysis, this localized domain is stable if the beam power J exceeds the threshold J_p. To estimate the latter, it is convenient to use the model[48] in which $\mu_\omega(T) = \mu_0$ for $T > T_c$ and $\mu_\omega(T) = 0$ for $T < T_c$, with the remaining parameters in (4.4) being independent of T (see also Sec. 2B). Neglecting light absorption, we obtain (see, for example, Ref. 48)

$$J_p = \frac{2\pi\gamma\varkappa}{c\mu_0}(T_c - T_0). \qquad (4.6)$$

This formula has a simple physical interpretation: the intensity of the incident radiation should be sufficient to heat up the plasma to a temperature of the order of T_c, i.e., $c\mu_0 P_p \sim (T_c - T_0)\gamma\varkappa/r^2$.

Let us now examine in greater detail the situation where, as a result of the focusing of the laser beam, the function $P(x)$ varies slowly over lengths of the order of r, i.e., $l_f \gg r$ (Fig. 18). In this case, we have the localization of the domain on a smooth ($\varepsilon \ll 1$) inhomogeneity. The domain dimensions D_+ and D_- can be determined from equations analogous to (2.22):

$$v[J(D_\pm), D_\pm] = 0, \qquad (4.7)$$

where the explicit dependence of the domain-wall velocity v on $D_\pm$ is due to the presence of the inhomogeneity (focusing), while the dependence of J on $D_\pm$ is connected with the absorption of radiation in plasma, which is assumed to be sufficiently weak ($\mu_\omega r \ll 1$). The veloicty v can be expressed in terms of the laser-beam and gas parameters, in accordance with (2.5). On the other hand, the equations given by (4.7) are themselves equivalent to the "equal areas theorem" (2.4), where $\beta \equiv J(x)$ and the coordinate x is a parameter.

When $D_\pm \ll l_f$, the equations given by (4.7) can be expanded into series in powers of $D_\pm$. If we place the origin at the focus, we obtain the equations describing the slow dynamics of the domain in the case of sufficiently weak absorption $\mu_\omega(T_2) l_f \ll 1$ [7)]

$$\frac{\partial D_-}{\partial t} = v_1(J) - sD_-^2, \qquad (4.8)$$

$$\frac{\partial D_+}{\partial t} = v_1(J) - m(D_+ + D_-) - sD_+^2, \qquad (4.9)$$

where J is the beam power incident on the left boundary ($x = -D_-$) of the domain (see Fig. 18) and $v_1(J)$ is the velocity of the plasma boundary (domain wall) along the uniform beam ($\varepsilon = 0$) with $J_p = J_p(0)$. The parameters s and m in (4.8) and (4.9) are given by

$$s = \frac{1}{2}\left|\frac{\partial^2 v}{\partial x^2}\right|_{x=0} \sim \frac{v_0}{l_f^2},$$

$$m = -\frac{\partial v}{\partial J}\frac{\partial J}{\partial x}\bigg|_{D_-} = J\mu_\omega(T_3)\frac{\partial v}{\partial J} \backsim \mu_0 v_0, \qquad (4.10)$$

where $v_0 \propto \varkappa/\nu r$ and we have used (4.5) in the derivation of the expression for m. We note that (4.8) and (4.9) are analogous to (2.19). The appearance in (4.9) of the additional term $-m(D_+ + D_-)$ is due to a reduction in the intensity of radiation reaching the right-hand wall of the domain ($x = D_+$) as a result of absorption of light.

The solutions of (4.8) and (4.9) that describe a stable localized domain can be readily obtained:

$$D_+ = \sqrt{\frac{v_1}{s}} - \frac{m}{s}, \quad D_- = \sqrt{\frac{v_1}{s}}. \qquad (4.11)$$

It is clear that the inclusion of absorption ($m > 0$) leads to an asymmetry of the domain ($D_- > D_+$). As the power J decreases, the domain length $D = D_+ + D_-$ is found to fall,

[7)]This case is characteristic, for example, for the neodymium laser in the case of a discharge in the atmosphere,[47] where $\mu_\omega(T_2) \approx 4\cdot 10^{-3}$ cm^{-1} for $T_2 \approx 12\,000$ K, $J_p \approx 1$ MW.[73]

since $v_1(J) \propto J - J_p(0)$ for $J \simeq J - J_p(0)$ [see (2.5)] and m, $s =$ const. When $v_1(J) < m^2/s$, the right-hand domain wall shifts to the left of the focus ($D_+ < 0$, see Fig. 18). When the power J becomes equal to J_r, where J_r is given by the condition $v_1(J_r) = m^2/4s$, the domain vanishes. We then have $D_+ = -D_-$, $D = 0$ and $J_r - J_p(0) \sim J_p(0) \cdot (\mu_0 l_f)^2$. The domain vanishes at the point $x = -D_c$, which lies to the left of the focus at a distance given by

$$D_c = \frac{m}{2s} \backsim \mu_\omega (T_2)\, l_f^2 \tag{4.12}$$

when we have used (4.10) to obtain an approximate estimate. Under the conditions of the experiment reported in Ref. 47, where $l_f = 50$ cm and $\mu_\omega(T_2) \approx 4 \cdot 10^{-3}$ (Ref. 48), the length D_c is of the order of 1–10 cm.

A similar approach can be used to examine, for example, a localized plasma column in a microwave discharge,[73] a glow discharge in a tube of variable cross section,[124] and so on. We note that, as in the above example, the inhomogeneity is then frequently due to the discharge geometry itself.

C. Temperature-electric domains in normal metals

We now consider one further example, namely, that of temperature-electric domains in a normal metal carrying a current. In an infinite specimen, such domains can be present if the heat-balance equation $\rho(T^2)j^2 = W(T)$ is satisfied for two or more values of the temperature T (see Fig. 4). In practice, this situation occurs either when the resistivity $\rho(T)$ is a sufficiently rapidly varying function of temperature, or when the heat-removal function $W = W(T)$ is N-shaped (Figs. 4a and b, respectively).

If, for example, the presence of three crossing points of the functions $Q(T)$ and $W(T)$ is largely due to the behavior of the resistivity $\rho(T)$, the appearance of a temperature domain is accompanied by the appearance of an essentially inhomogeneous electric field. Domains of this kind are essentially temperature-electric domains.[41] Let us examine the physical mechanisms responsible for the appearance of such domains. The function $Q = Q(T)$, similar to that shown in Fig. 4a, is characteristic for any sufficiently pure metal because the transition from helium to nitrogen temperatures is accompanied by the onset of phonon scattering of electrons, which gives rise to a substantial[41] increase in $\rho(t)$. Moreover, the appearance of the temperature-electric domains may be connected with phase transformations, in which case $\rho(T)$ increases[42] in narrow temperature intervals.[8)] For example, this may occur in melting, during magnetic transitions,[39,43] and so on. As far as the N-shaped function $W = W(T)$ is concerned, this may be due to the particular features of the electron-phonon interaction, for example, the presence of a "narrow phonon bottleneck" in semi-metals,[126] and so on.

So far, we have been concerned with the properties of a metal as such. On the other hand, the properties of the cooling medium may undergo a change when the heat flux leaving the specimen for the coolant is high. A characteristic example of this is the so-called boiling crisis of a liquid coolant,[70,71] i.e., the transition from bubble to film boiling (see Fig. 4b). The result of this is that, when heat is removed by a boiling liquid temperature-electric domains due to the formation of a vapor film on the surface of the metal[127,128] may appear. At constant current, the transition of the metal from one homogeneous state ($T = T_1$) to another ($T = T_3$) occurs for $j > j^*$ (see Fig. 4a). If, on the other hand, the voltage rather than the current is constant, this transition cannot occur because it is accompanied by a rapid increase in resistivity and a reduction in j below the value j_* for which there is no equilibrium state with $T = T_3$. Thus, only a portion of the specimen can go over into the high-temperature state, and it is this portion that constitutes the temperature-electric domain.

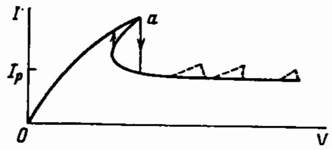

FIG. 19. Current-voltage characteristic of a normal metal with a temperature-electric domain. Broken line shows the change in the CVC in the presence of point inhomogeneities.

Figure 19 shows the CVC of a metal containing a temperature-electric domain (see, for example, Refs. 42 and 129). The branch $0a$ corresponds to a uniformly heated metal ($T = T_1$), whereas the remainder of the characteristic corresponds to a specimen containing a domain. When the voltage V is high enough, the current I in the metal remains constant (barretter effect[42]). The length $D(V)$ of the domain is then determined from the condition for the equilibrium of its boundaries $I = I_p$, i.e.,

$$R_0(I_p)\, I_p + \Delta\rho\, (I_p)\, D\, (V)\, I_p = V, \tag{4.13}$$

where $R_0(I)$ is the resistance of the specimen with $T = T_1(I)$, and $\Delta\rho$ is the jump in the resistance of a specimen of unit length in a transition from the state with $T = T_1$ to the state with $T = T_3$.

Domains may become localized in inhomogeneous metals, which will lead to the following effects: (1) stabilization of the domain at constant current, (2) existence of several types of localized domain and, consequently, the presence of discontinuous transitions between them when I changes, when external perturbations are introduced, and so on, and (3) multivaluedness, steps, and hysteresis on the CVC.

As an example, let us consider the segment of the CVC for a homogeneous specimen on which the current is stabilized ($I = I_p$) (see Fig. 19) and an increase in V produces a proportional increase in the domain length $D(V)$ [see (4.13)]. When local inhomogeneities are present, this situation will continue until both domain boundaries encounter "cold" inhomogeneities ($\Gamma < 0$). As shown in Sec. 2, this leads to the localization of domain walls. As a result, the domain will be "held" between two inhomogeneities, and its length will cease to be a function of V. The CVC of a specimen with this type of localized domain will be resistive, so that further increase in V will produce a rise in the current I until one of

---

8) If $\rho(T)$ decreases with increasing T, the phases may separate in the direction perpendicular to the current, and filaments will be formed (examples are the melting of gallium, antimony, and bismuth, the transition from the ferromagnetic to the superconducting state in magnetic superconductors,[125] and so on.

the domain walls detaches itself from the inhomogeneity $[I - I_p > \Delta I \sim |\Gamma| I_p$; see also (2.17)]. When the domain walls become delocalized, there is a discontinuous change in the current by the amount ΔI, and the specimen goes over into the barretter state[42] until, with increasing V, the domain boundary meets the next inhomogeneity with $\Gamma < 0$. Thus, the CVC of an inhomogeneous specimen assumes the saw-tooth shape (broken curve in Fig. 19). We note that the separation between the "teeth" on the CVC is uniquely related to the separation between the inhomogeneities in the specimen.

Temperature-electric and thermal domains have been observed[42,128–131] at different coolant temperatures, and localized thermal domains were reported in Ref. 128.

D. Chemical-reaction waves

We shall now illustrate in detail the situation that arises during the localization of a domain wall by considering the example of switching waves that accompany chemical reactions. We shall examine two limiting cases, namely, nonisothermal waves propagating over the surface of a solid catalyst[51–52] and isothermal waves accompanying the "cold combustion" chain reaction (Refs. 49, 50, 54, and 132). Suppose that a chemical reaction between gaseous reagents occurs on the surface of a thin catalyst wire of diameter d. Depending on its temperature, the catalyst can be in one of two reactive states, namely, the kinetic state (low temperature) and highly-active diffusion state (high temperature; see, for example, Ref. 49). The switching of the catalyst activity states occurs through the propagation of a temperature wave[51,52] which can be described by

$$\nu \frac{\partial T}{\partial t} = \varkappa \frac{\partial^2 T}{\partial x^2} - \frac{4}{d} \left[h (T - T_0) - CmQ\theta (T - T_k) \right], \tag{4.14}$$

where ν and $\varkappa$ are the specific heat and thermal conductivity of the catalyst, h is the heat-transfer coefficient between the wire and the ambient gas at temperature T_0, m is the mass supply coefficient for a reagent of concentration C, Q is the heat of the reaction, and $T_k \sim E_a$, where E_a is the reaction activation energy. For simplicity, ν, $\varkappa$, and h are assumed temperature-independent in (4.14), and heat release in the kinetic state has been neglected ($T < T_k$).

Let us now consider the localization of the switching wave for the catalyst activity state on an inhomogeneity due to, for example, a local rise in $h(x)$ over a length $2l$. It will be convenient to write (4.14) in dimensionless form by substituting $x_1 = x/L$, $t_1 = t/\tau$, and $\psi = (T - T_0)/(T_k - T_0)$, where $L = \sqrt{d\varkappa/4h}$ and $\tau = \nu d/4h$. We then have

$$\dot{\psi} = \psi'' - \psi + \beta\theta(\psi - 1) + \Gamma\psi\delta(x_1), \tag{4.15}$$

where

$$\beta = \frac{CmQ}{(T_k - T_0) h}, \quad \Gamma = \int_{-l}^{l} \left[1 - \frac{h(x)}{h} \right] \frac{dx}{L}. \tag{4.16}$$

We note that (4.15) is a special case of (2.24), which we investigated in Sec. 2C.

When $\Gamma = 0$, we can readily find the solution describing the domain wall moving with velocity v from Eq. (4.15), where

$$v = v_0 \frac{\beta - 2}{\sqrt{\beta - 1}}. \tag{4.17}$$

It is clear from the last equation that the two-phase state can exist only when $\beta > 1$. For $l < \beta < 2$, the domain wall takes the catalyst from the diffusion state to the kinetic state, and the reverse situation occurs for $\beta > 2$. If, on the other hand, $\beta = 2$, the domain wall is at rest ($\beta_p = 2$).

It is readily shown from (4.15) [see also (2.17)] that, when $\Gamma < 0$, the diffusion-state wave is localized in the range $\beta_p < \beta < \beta_2$, where, for $|\Gamma| \ll 1$, we have

$$\beta_2 = 2 - \Gamma. \tag{4.18}$$

Since, for each value of β, there is a wave moving with a particular velocity $v = v(\beta)$, it follows from (4.18) that the diffusion-state waves with velocities $v < v_k$ ($v_k = v(\beta_2)$) cannot propagate. The magnitude of the critical velocity can be found from (4.17) and (4.18): $v_k = 2|\Gamma| v_0$, ($|\Gamma| \ll 1$). We note that $\Gamma \propto d^{-1/2}$, so that the importance of the inhomogeneities increases with increasing d.

If, for example, the velocity is investigated experimentally as a function of the temperature T_0 of the medium, it is found that the wave will not propagate for $T_p < T_0 < T_p + \delta T_0$. The temperature T_p is determined from the relation $\beta(T_p) = \beta_p = 2$, and

$$\delta T_0 = (T_k - T_0) \, |\Gamma|. \tag{4.19}$$

We note that, in the range $T_p < T_0 < T_p + \delta T_0$, the catalyst can go over into a metastable inhomogeneous state, so that segments of kinetic and diffusion states will alternate along its length, and the combustion process will occur in "spots."

Effects associated with the localization of chemical-reaction waves on the surface of a catalyst have often been seen experimentally.[51,52,133] In particular, localization of waves moving with velocities $v < v_k$ has been observed in the course of experiments involving the oxidization of CO, ammonia, and ethylene[51,52,133] on platinum. A series of alternating localized regions in different reaction states has been obtained by producing artificial inhomogeneities.[51,52]

Figure 20 shows the temperature profile of a moving (1) and localized (2) wave during the oxidation of ethylene on platinum.[133] There is a clear "knee" that is characteristic for waves localized on inhomogeneities (cf. Fig. 7). It is found[51] that, when ammonia is oxidized on platinum, $T_k - T_0 \sim 1000$ K and the localization interval is $\delta T_0 \sim 10$

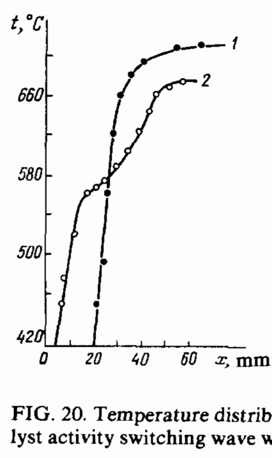

FIG. 20. Temperature distribution in a moving (1) and localized (2) catalyst activity switching wave when ethylene is oxidized on platinum.[133]

K. It follows from (4.19) that a small inhomogeneity with $\Gamma \sim 0.01$ is sufficient to localize the waves under the conditions prevailing in the experiment described in Ref. 51.

Let us now examine the isothermal "cold" combustion reaction which can occur in a gaseous medium (see, for example, Refs. 49, 50, and 132), on the surface of a catalyst,[54] and so on. During "cold" combustion, there is a deficiency of one of the reagents, the heating of the mixture by the heat of the reaction is small, and hence the propagation of the usual combustion waves associated with thermal self-ignition[49,50] is not possible. Recently, there has been increased interest in such reactions in connection with the development of chemical lasers.[134]

The "cold" combustion reaction proceeds through a series of intermediate stages, one of which involves the formation of active centers that are responsible for chain branching. This leads to the propagation of "cold" combustion waves due to the diffusion of active centers.[50] Let us consider the localization of such waves when they are associated with, for example, an inhomogeneity on the surface of a reaction tube or catalyst.

When the active centers have long lifetimes, the initial set of equations describing the chemical kinetics of the system can be reduced to a single diffusion equation for the concentration n of the active centers:

$$\frac{\partial n}{\partial t}=D_n\frac{\partial^2 n}{\partial x^2}-f(n), \tag{4.20}$$

where the specific form of $f(n)$ is determined by the nature of the intermediate stages of the given reaction and, for simplicity, the diffusion coefficient D_n is assumed to be independent of n.

We shall confine our attention to the case of quadratic chain branching so that $f(n)$ is of the form[49,50,132]

$$f(n)=kn-\frac{k_1n^2(n_0-n)}{k_2+mk_3}, \tag{4.21}$$

where k and k_1 are constants that can be expressed in terms of the corresponding rate constants for the elementary reactions, m is the concentration of molecules M on which the reaction chain stops, n_0 is the initial concentration of the deficient reagent, and k_2 and k_3 are rate constants representing chain breaking at the wall of the reaction tube and as a result of a collision with the molecule M, respectively.

Equation (4.21) provides a sufficiently satisfactory description of, for example,[132] the oxidation of CS_2 ($n_0=[CS_2]$, oxygen in surplus).

Equation (4.20) is analogous to (2.6) with $U=U(n)$ similar to that shown in Fig. 3. It will be convenient to transform to dimensionless variables $x_1=x/L$, $t_1=t/\tau$, $y=n/n_0$, where $L=\sqrt{D_n/k}$ and $\tau=k^{-1}$, and take the intensive parameter β in the form $\beta=k_1n_0^2/k\ (k_2+mk_3)$. The "cold" combustion waves will then be the above domain walls. They can obviously exist only for $n_0>n_p$; for $n_0=n_p$ the wave velocity is zero, and for $n_0<n_p$ the propagation of such waves is impossible. The quantity n_p is found from the equation $\beta_p=9/2$ (see, for example, Ref. 50).

Let us now consider the localization of the "cold" combustion wave on an inhomogeneity connected with a local increase in the rate k_2 of chain-breaking on the tube wall over a length $2l \ll L$. As shown in Sec. 3, the condition for this localization is the existence of nontrivial solutions y_m and of Eqs. (3.5) and (3.6), which in our case ($\psi_m\equiv y_m$), take the form

$$\frac{\beta-\beta_p}{\beta_p}=\frac{81}{4}\Gamma y_m^3(1-y_m)\left(1-\frac{3}{2}y_m\right), \tag{4.22}$$

$$\Gamma=\int_{-\infty}^{\infty}\frac{k_2(x)-k_2(\infty)}{k_2(x)+mk_3}dx_1, \tag{4.23}$$

where $\Gamma\sim l/L$ and terms of the order of Γ^2 are neglected in (4.22). The critical quantity β_2, for which the localization of the combustion wave takes place, can be found from (4.22):

$$\beta_2=\beta_p+c_1\Gamma,\qquad c_1=\frac{9}{10}\left(1-\frac{1}{\sqrt{10}}\right)^3\left(1+\frac{2}{\sqrt{10}}\right)\approx 1{,}49. \tag{4.24}$$

The critical velocity v_k can be readily obtained by substituting for β_2 in (2.5). This yields

$$v_k=c_2k\int_{-\infty}^{\infty}\frac{k_2(x)-k_2(\infty)}{k_2(x)+mk_3}dx,\quad c_2=\frac{2}{3}c_1\approx 1. \tag{4.25}$$

Thus, the flame becomes extinguished before the wave velocity becomes equal to zero, and this had already been seen in early experiments on the "cold" oxidation of CS_2 (an alternative explanation is given in Ref. 135).

Direct measurements of v_k yield information on the kinetics of the intermediate stages of "cold" combustion regions. In particular, if a region with $k_2 \gg \max[k_2(\infty), mk_3]$ is artificially produced on the surface of the reaction tube, then $v_k\approx 2lk$, so that the constant k can be investigated as a function of T and of pressure. When the constant k corresponds to a second-order reaction,[132] we have

$$v_k\approx 2lk_0\left(\frac{p}{p_0}\right)\exp\left(-\frac{E_a}{RT}\right), \tag{4.26}$$

where p is the partial pressure of oxygen and E_a is the activation energy (the temperature dependence of the preexponential factor k_0 is neglected).

E. Superconductor exposed to laser radiation

Superconducting and resistive phases, and also superconducting phases with different values of the modulus of the order parameter Δ (see, for example, Ref. 62), can coexist in a superconductor exposed to a laser beam. The nonlinear waves (domain walls) in which we are interested are the separation boundaries between the corresponding phases. Waves of this type are usually connected with the diffusion of nonequilibrium electronic excitations and are described by equations such as (4.20),[62] where the function $U=U(n)$ is analogous to that shown in Fig. 3, and the parameter β is replaced by the radiation power P.

When a certain threshold power P_p is exceeded, the resistive phase replaces the superconducting phase and, for $P\simeq P_p$, the velocity of the N–S boundary is $v\sim P-P_p$. The quantity P_p can be estimated by equating the density n_R of Cooper pairs broken up by the electromagnetic field to the equilibrium density of paired electrons $n_0\sim\Delta^2N_F/k_BT_c$, where N_F is the density of states on the Fermi surface and k_B is the Boltzmann constant. We also have $n_R\sim N_R\tau_\varepsilon r/d$, where N_R is the number of photons absorbed by a unit surface of the film per unit time, τ_ε is the electron energy relaxation time, r is a coefficient representing the multiplication of quasiparticles due to reabsorption of phonons, collisional ionization across the gap, and so on,[62] and d is the film thickness. The above estimate for n_R has a simple physical interpretation: each absorbed photon results in the breaking up of r Cooper pairs, so that $2r$ nonequilibrium quasiparticles are produced and recombine in a time τ_ε. Since $N_R = (1-k)P/\hbar\omega$, where ω is the radiation frequency and k is the reflection coefficient, it follows from the foregoing estimates that[62,136]

$$P_p \sim \frac{\Delta^2 \hbar\omega N_F d}{(1-k)\tau_\varepsilon r k_B T_c}, \tag{4.27}$$

where $\Delta^2 \sim T_c(T_c - T_0)k_B^2$.

In the case of time-independent illumination with power $P > P_p$, the entire specimen goes over to the resistive state in a time L_{sp}/v, where L_{sp} is the specimen length. Under pulsed illumination,[97-99] the resistive phase exists only during the pulse length $\tau_0(\tau_0 \gg \tau_\varepsilon)$, and the size of the region occupied by it is of the order of $v\tau_0$ (this is the model of the dynamic intermediate state[137]).

The presence of inhomogeneities in the superconductor may lead to the following. Firstly, the resistive phase may become localized under stationary illumination. Secondly, in the case of pulsed illumination, localization of the domain walls can occur, and this will lead to a deviation of the observed resistance R from the relation $\rho v\tau_0/A$ predicted by the model of the nonstationary inhomogeneous state. Localization of the resistive phase on inhomogeneities can, in turn, be accompanied by hysteresis effects similar to those described above.

Characteristic inhomogeneities can be due to, for example, variable film thickness, the nature of the surface, the distribution of impurities in various structural defects, the illumination itself (controlled weak coupling[138]), and so on. We note that some of the inhomogeneities on which the localization of domain walls is possible have no essential effect on the width of the superconducting junction, which is usually a measure of the inhomogeneity of a superconductor. This applies, for example, to point inhomogeneities (because of the smallness of the ratio l/L_{sp}), the inhomogeneous distribution of nonmagnetic impurities that do not affect T_c by virtue of the Anderson theorem,[96] the surface properties that produce a change in the reflection coefficient k in (4.27), and so on.

Thus, the resistive states of films that are homogeneous in the sense of the width of the superconducting junction, which appear under time-independent laser illumination, can be determined by the localization of N–S boundaries on inhomogeneities.

F. Dielectric-metal phase transition

Let us now consider the nonlinear waves that accompany the dielectric-metal phase transition (see, for example, Ref. 139). This transition usually occurs when the temperature or pressure is increased, and is accompanied by a large (by ten orders of magnitude in vanadium oxides) jump in the conductivity and a radical change in optical properties,

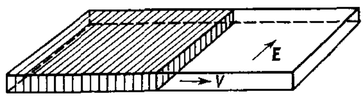

FIG. 21. Phase separation across a metal-dielectric transition in an electric field **E**.

which is widely exploited in electronics, optoelectronics, and so on.[139]

The nonlinear waves in which we are interested arise under nonequilibrium conditions and, in particular, when the specimen is heated by an electromagnetic field,[64,139] when a nonequilibrium distribution of carriers is established,[63] and so on. They are switching waves that take the specimen from the metal to the dielectric state and back again. To be specific, we shall consider temperature waves (domain walls) that arise in a constant electric field E[64,139] where, obviously, the heat release in $Q = \sigma(T)E^2$. Since in contrast to, for example, a superconductor carrying a current, the system in which we are interested does not have an N- or S-shaped CVC, the phase separation within it occurs at right-angles to the direction of the E-lines[17,18] (Fig. 21). In all other respects, the switching waves are analogous, in this case, to those considered above (see Chap. 2). For example, the function $U(T)$ is similar to that shown in Fig. 3, where E plays the role of the parameter β.

The velocity of the switching wave (domain wall) changes sign at $E = E_p$. The quantity E_p can be readily estimated by analogy with (4.3) (see also Ref. 64):

$$E_p \sim \sqrt{\frac{hT_c}{\sigma d}}\sqrt{1-\frac{T_0}{T_c}}, \tag{4.28}$$

where σ is the conductivity of the metal phase and T_c is the phase transition temperature. When $E > E_p$, the metal phase replaces the dielectric phase, and the reverse situation occurs for $E < E_p$.

The presence of inhomogeneities ensures that the domain wall can be localized for $E \simeq E_p$. In particular, for conductivity inhomogeneities, we have $E_2 - E_p \sim \Gamma E_p$, where $\Gamma \sim \Delta\sigma l/\sigma L$, $L = \sqrt{d\varkappa/h}$, $\Delta\sigma = \sigma - \sigma_0$. As an example, consider the propagation of the switching wave in a medium with point inhomogeneities for $E > E_p$. We shall use the simple model discussed in Sec. 2, and take into account the inhomogeneity by adding the terms $\Sigma_i \Gamma_i \delta(x - x_i)$ to the right-hand side of (2.24), where Γ_i are constants characterizing the strength of the i-th inhomogeneity at $x = x_i$.

Equation (2.44) describes the dynamics of the domain wall in our case and can be integrated readily, so that the motion of the wall can be determined for an arbitrary distribution of inhomogeneities. To illustrate the situation, we shall confine our attention to the limiting case $|x_i - x_{i\pm 1}| \gg L$, where the wave front interacts with each inhomogeneity separately. The wave then propagates in stages, accelerating as it passes inhomogeneities with $\Gamma_i > 0$ and decelerating when $\Gamma_i < 0$. The dynamics of such processes is described by (2.43), in which $t \equiv |t|$.

We shall now establish an expression for the mean velocity of a domain wall, $\bar{v} = L_{sp}/\bar{t}$, where $\bar{t}$ is the time taken by the wave to traverse the entire specimen. It is clear that

$\bar{t} = (L_{sp}/v) + \Sigma_i \Delta t_i$, where Δt_i is the time by which the domain is delayed on the i-th inhomogeneity and $v = v(E)$ is its velocity in a homogeneous specimen ($v > 0$ for $E > E_p$). We can readily show from (2.43) that $\Delta t_i = -(2L/v)\ln[1 + (2\Gamma_i v_0/v)]$, where $v_0 = L/\tau$, and $\tau = vd/h$ is the thermal time. We now introduce the inhomogeneity distribution function $\varphi(\Gamma)$ and obtain

$$\bar{t} = \frac{L_{sp}}{v}\left[1 + \frac{2L}{l_i}\int_{-\infty}^{\infty} d\Gamma\varphi(\Gamma)\ln\frac{v}{v+2\Gamma v_0}\right], \quad (4.29)$$

where l_i is the mean separation between inhomogeneities ($l_i \gg L$). The time t becomes infinite in the presence of at least one inhomogeneity Γ_i for which the localization condition $2v_0|\Gamma_i| > v$ is satisfied. If, for example, the inhomogeneities are identical sources or sinks of heat ($|\Gamma_i| = \Gamma_0$), and the specimen is homogeneous on average ($\Sigma_i\Gamma_i = 0$), then

$$\bar{v} = \frac{v}{1 + \frac{L}{l_i}\ln\frac{v^2}{v^2 - 4\Gamma^2 v_0^2}}. \quad (4.30)$$

The quantity $\bar{v}$ vanishes at the localization threshold ($2\Gamma_0 v_0 = v$). When this is so, and $v - 2\Gamma_0 v_0 > \delta v \sim v_0\Gamma \times\exp(-l_i/L)$, the inhomogeneities have practically no effect on the mean wave velocity.

Thus, the inhomogeneities influence the switching time (especially for $E \simeq E_p$), and this may be important in applications. We note that, by suitably introducing artificial inhomogeneities, it is possible to produce metallic regions (current filaments), localized in the dielectric phase. In particular, the CVC hysteresis and the discontinuous transitions between different states of localized waves that were discussed above can be used to record and store information, and so on.

G. Dissipative structures in an inhomogeneous medium

In the preceding sections, we were largely concerned with localized states of domains and domain walls on *isolated* inhomogeneities. If, on the other hand, the specimen contains several inhomogeneities, they may combine into a metastable inhomogeneous state in the form of a structure consisting of individual fragments in the form of localized domains or domain walls. Let us consider the properties of such structures in greater detail.

We begin with the relatively simple case of smooth inhomogeneities, for which the most important factor is the variation in $\beta_p = \beta_p(x)$ along the specimen. Stable "strong-field" domains can then localize on inhomogeneities in the neighborhood of the minima of the function $\beta_p(x)$. If, for example, such domains are described by the thermal conduction equation (2.6), the resulting structure takes the form of a sequence of alternating "hot" and "cold" phases. We note that, for a given distribution of inhomogeneities, the form of the structure itself is not uniquely determined by the magnitude of β. In fact, a finite-amplitude fluctuation is, in general, necessary for the formation of each localized domain. The maximum number of different structures that can be realized in the presence of n smooth inhomogeneities is equal to 2^n. The specific form of the resulting structure is

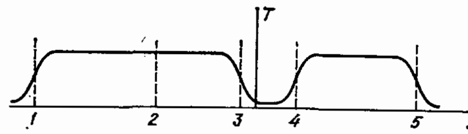

FIG. 22. Example of a dissipative structure arising during localization of domain walls on inhomogeneities 1, 2, 3, 4, and 5.

then determined by the prior history of the specimen, the nature of external agencies, and so on.

A variation in the parameter β may be accompanied by sudden rearrangement of the above structures, for example, as a result of a "hop" of the domain boundary to a neighboring inhomogeneity, the appearance of new localized domains, and so on. As already noted above, such a rearrangement is usually accompanied by hysteresis (see Fig. 10).

A metastable multiphase structure due to the localization of either interphase boundaries (domain walls) or regions of different phase of finite dimensions (domains) may exist in the presence of point inhomogeneities. For example, the localization of domain walls in the specimen may be accompanied by the presence of regions of different phase, whose dimensions D_n are determined by the separation between the inhomogeneities (Fig. 22). When the localization condition (3.5) is satisfied for each of the domain walls, the quantity D_n is a slowly-varying function of β. When this condition ceases to be satisfied for some particular inhomogeneity, for example, inhomogeneity 1 in Fig. 22, the domain wall localized upon it "breaks off", and the length of the left domain in Fig. 22 decreases until the wall meets a stronger inhomogeneity along its path, for example, inhomogeneity 2. This discontinuous rearrangement can occur both as a result of a change in β and in response to a strong enough external perturbation. We note that hysteresis connected with the difference between β_p and β_2 (see Chap. 2) will occur when the variation in β is reversed.

The foregoing considerations can also be used to describe dissipative structures in an inhomogeneous medium. Thus, dissipative structures such as static spatially inhomogeneous distributions of various physical quantities (concentrations of chemical reagents, density, electric field, temperature, and so on) that appear under nonequilibrium conditions are usually described by the two coupled equations (see, for example, Refs 4–6):

$$\nu_\psi\frac{\partial\psi}{\partial t} = \frac{\partial}{\partial x}\varkappa_\psi\frac{\partial\psi}{\partial x} - f(\psi, \varphi), \quad (4.31)$$

$$\nu_\varphi\frac{\partial\varphi}{\partial t} = \frac{\partial}{\partial x}\varkappa_\varphi\frac{\partial\varphi}{\partial x} - \Phi(\psi, \varphi), \quad (4.32)$$

where the variables $\psi(x,t)$ and $\varphi(x,t)$ are determined by the nature of the particular problem. The functions $f(\psi,\varphi)$ and $\Phi(\psi,\varphi)$ describe the interaction (including self-interaction) of the quantities ψ and φ.

Dissipative structures (periodic, stochastic, and so on) in various physical, chemical, and biological systems have attracted considerable attention in recent years (see, for example, Refs. 1–6, 32, 33, and 140). The necessary condition for the appearance of such structures in a homogeneous medium is that the zero isocline $\varphi = \varphi_s(\psi)$ of Eq. (4.31)

($f(\psi,\varphi_s) = 0$) should be N-shaped (compare with Fig. 2) and the variable $\varphi(x,t)$ should damp the inhomogeneous distributions $\psi(x)$ (for example, periodic, etc.[4,140]) that are stable for φ = const. In this approach, the medium in which the dissipative structures appear is itself only a passive background on which "the action" takes place. On the other hand, inhomogeneities are alway present in real systems in one form or another.

The foregoing discussion shows that the presence of the damping variable $\varphi(x,t)$ is not a necessary condition for the existence of a dissipative structure in an inhomogeneous medium: its functions begin to be performed by the inhomogeneity. The formal transition from (4.31) and (4.32) to (2.6), which describes an inhomogeneous one-component medium ($\mu \equiv 0$), occurs when the function $\Phi(\psi,\varphi)$ is independent of ψ, i.e., the variable $\varphi(x,t)$ plays the role of a given external field. We now list the leading features of the above dissipative structures: (1) hard excitation regime, (2) discontinuous rearrangement and hysteresis accompanying a variation in the external parameters, and (3) essential dependence of characteristics on the disposition and strength of inhomogeneities which, in a sense, may be looked upon as data-carrying "nuclei" in the dissipative structure (see, for example, Ref. 4).

When the function $\Phi(\psi,\varphi)$ in (4.32) varies appreciably with ψ, the variable $\varphi(x,t)$ may be looked upon as a self-consistent inhomogeneity that adjusts itself to the field $\psi(x,t)$. If the characteristic spatial scales L_ψ and L_φ of Eqs. (4.31) and (4.32) are essentially different, the resulting dissipative structures can be usefully analyzed by the methods presented above as applied to inhomogeneous one-component systems. Finally, as far as the effect of true inhomogeneities on the properties of multicomponent dissipative structures, described, for example, by Eqs. (4.31) and (4.32), is concerned, this problem is, of course, of independent interest (see, for example, Refs. 141 and 142 and the review given in Ref. 143).

5. CONCLUSIONS

We have attempted in this review to delineate the general features of nonlinear waves such as domains and domain walls localized on inhomogeneities of a medium. Our analysis shows that this localization can have an important effect on different physical properties of the system.

The waves considered in this review corresponded to one-dimensional or, more precisely, quasi-one-dimensional situations that are relatively frequently encountered in experiments. The description of two- and three-dimensional waves localized on inhomogeneities is an undoubtedly important but more complex problem. However, the recently developed very effective methods of integrating nonlinear partial differential equations, based, for example, on the inverse scattering method,[9,10] lead us to the expectation that progress will be achieved in this area as well.

[1]Avtovolnovye protsessy v sistemakh s diffuzieĭ (Self-Wave Processes in Systems with Diffusion), ed. by M. T. Grekhova, Gor'kiĭ, 1981.
[2]V. A. Vasil'ev, Yu. M. Romanovskiĭ, and V. G. Yakhno, Usp. Fiz. Nauk **128**, 625 (1979) [Sov. Phys. Usp. **22**, 615 (1979)].
[3]A. C. Scott, Waves in Active and Nonlinear Media and Their Application in Electronics [Russ. Transl. Sov. Radio, Moscow, 1977].
[4]G. Nicolis and I. Prigogine, Self-Organization in Nonequilibrium Systems, Wiley-Interscience, N.Y. 1977 [Russ. Transl., Mir, Moscow, 1979].
[5]W. Ebeling, Evolution of Structures in Irreversible Processes, Mir, Moscow, 1977.
[6]G. Haken (ed.), Synergetics, Springer Verlag, Berlin, 1977 [Russ. Transl., Mir, Moscow, 1980].
[7]C. Cercignani, Rev. Nuovo Cimento **7**, 429 (1977).
[8]Solitons in Action, ed. by K. E. Longren and A. C. Scott, Academic Press, N.Y. 1978 [Russ. Transl., Mir, Moscow, 1981].
[9]C. S. Gardner, J. M. Green, M. D. Kruskal, and R. M. Miura, Phys. Rev. Lett. **19**, 1095 (1976).
[10]V. E. Zakharov, S. V. Manakov, S. P. Novikov, and L. P. Pitaevskiĭ, Teoriya solitonov: Metod obratnoĭ zadachi (Theory of Solitons: The Methods of Inverse Scattering), Nauka, Moscow, 1980.
[11]G. M. Zaslavskiĭ, Usp. Fiz. Nauk **111**, 395 (1973) [Sov. Phys. Usp. **16**, 761 (1974)].
[12]M. B. Fogel, S. E. Trullinger, A. R. Bishop, and J. A. Krumhansl, Phys. Rev. B **15**, 1578 (1977).
[13]I. O. Kulik and I. K. Yanson, Effekt Dzhozefsona v sverkhprovodyashchikh tunnel'nykh strukturakh (Josephson Effect in Superconducting Tunnel Structures), Nauka, Moscow, 1970.
[14]K. K. *Likharev and B. T. Ul'rikh, Sistemy s dzhozefsonovskimi kontaktami* (Systems With Josephson Contacts), Moscow University, 1978.
[15]S. A. Vasenko, K. K. Likharev, and V. K. Semenov, Zh. Eksp. Teor. Fiz. **81**, 1444 (1981) [Sov. Phys. JETP **54**, 768 (1981)].
[16]Yu. S. Gal'pern and A. T. Filippov, Pis'ma Zh. Eksp. Teor. Fiz **35**, 470 (1982) [JETP Lett. **35**, 580 (1982)].
[17]A. F. Volkov and Sh. M. Kogan, Usp. Fiz. Nauk **96**, 633 (1968) [Sov. Phys. Usp. **11**, 881 (1969)].
[18]V. L. Bonch-Bruevich, I. P. Zvyagin, and A. G. Mironov, Dommenaya elektricheskaya neustoĭchivost' v poluprovodnikakh (Electrical Domain Instability in Semiconductors), Nauka, Moscow, 1972.
[19]A. F. Volkov and Sh. M. Kogan, Pis'ma Zh. Eksp. Teor. Fiz. **19**, 9 (1974) [JETP Lett. **19**, 4 (1974)].
[20]W. J. Skocpol, M. R. Beasley, and M. Tinkham, J. Appl. Phys. **45**, 4054 (1974).
[21]A. V. Gurevich and R. G. Mints, Pis'ma Zh. Eksp. Teor. Fiz. **31**, 52 (1981) [JETP Lett. **31**, 48 (1981)].
[22]R. G. Mints, Dokl. Akad. Nauk SSSR **248**, 352 (1979) [Sov. Phys. Dokl. **24**, 757 (1979)].
[23]A. B. Gurevich and R. G. Mints, Fiz. Tverd. Tela (Leningrad) **23**, 113 (1981) [Sov. Phys. Solid State **23**, 57 (1981)].
[24]A. V. Gurevich, Fiz. Tverd. Tela (Leningrad) **24**, 1776 (1982) [Sov. Phys. Solid State **24**, 1010 (1982)].
[25]P. A. Lee, T. M. Rice, and P. W. Anderson, Solid State Commun. **14**, 703 (1974).
[26]W. L. McMillan, Phys. Rev. B **14**, 1496 (1976).
[27]Yu. M. Ivanchenko, P. N. Mikheenko, and V. F. Khirnyĭ, Zh. Eksp. Teor. Fiz. **77**, 952 (1979) [Sov. Phys. JETP **50**, 479 (1979)]; **80**, 171 (1981) [**53**, 86 (1981)].
[28]Yu. M. Ivanchenko and P. N. Mikheenko, Zh. Eksp. Teor. Fiz. **82**, 488 (1982) [Sov. Phys. JETP **55**, 281 (1982)].
[29]N. N. Rozanov, Zh. Eksp. Teor. Fiz. **80**, 96 (1981) [Sov. Phys. JETP **53**, 47 (1981)].
[30]A. M. Nechaev, E. A. Rubakha, and V. F. Sinkevich, Radiotekh. Elektron. **26**, 1773 (1981).
[31]A. V. Nedospasov and V. D. Khait, Kolebaniya i neustoĭchivosti nizkotemperaturnoĭ plazmy (Oscillations and Instabilities of Low-Temperature Plasmas), Nauka, Moscow, 1979.
[32]Yu. M. Romanovskiĭ, N. V. Stepanova, and D. S. Chernavskiĭ, Matematicheskoe modelirovanie v biofizike (Mathematical Simulation in Biophysics), Nauka, Moscow, 1975.
[33]V. S. Markin, V. F. Pastushenko, and Yu. A. Chizmadzhev, Teoriya vozbudimykh sred (Theory of Excitable Media), Nauka, Moscow, 1981.
[34]M. A. Mikulinskiĭ, Usp. Fiz. Nauk **110**, 213 (1973) [Sov. Phys. Usp. **16**, 361 (1974)].
[35]A. P. Levanyuk, V. V. Osipov, A. S. Sigov, and A. A. Sobyanin, Zh. Eksp. Teor. Fiz. **76**, 34 (1979) [Sov. Phys. JETP **49**, 17 (1979)].
[36]J. W. Breemer and V. L. Newhouse, Phys. Rev. Lett. **1**, 282 (1958).
[37]B. I. Maddok, G. B. James, and W. T. Norris, Cryogenics, **9**, 261 (1969).
[38]W. C. Overton, J. Low Temp. Phys. **5**, 397 (1971).
[39]B. Ross and J. D. Lister, Phys. Rev. A **15**, 1246 (1977).
[40]R. Landauer, *ibid.* p. 2117.
[41]A. M. Kadigrobov and A. A. Slutskin, Pis'ma Zh. Eksp. Teor. Fiz. **28**, 219 (1978) [JETP Lett. **26**, 335 (1978)].
[42]V. V. Barelko, V. M. Beibutyan, Yu. E. Volodin, and Ya. B. Zel'dovich,

Dokl. Akad. Nauk SSSR **257**, 339 (1981) [Sov. Phys. Dokl. **26**, 335 (1981)].
[43]M. Ausloos, Physica (Utrecht) B **108**, 969 (1981).
[44]E. N. Rumanov, Zh. Eksp. Teor. Phys. **74**, 1422 (1978) [Sov. Phys. JETP **47**, 744 (1978)]; Pis'ma Zh. Eksp. Teor. Fiz. **35**, 286 (1982) [JETP Lett. **35**, 354 (1982)].
[45]B. N. Atrazhev and I. T. Yakubov, Teplofiz. Vys. Temp. **18**, 16 (1980).
[46]E. P. Velikhov and A. M. Dykhne, V kn. Trudy VII Mezhdunarodnogo simpoziuma po ionizatsionnym yavleniyam v gazakh (Proc. Seventh Intern. Symposium on Ionization Phenomena in Gases), Belgrade, 1965, p. 43.
[47]F. V. Bunkin, V. I. Konov, A. M. Prokhorov, and V. B. Fedorov, Pis'ma Zh. Eksp. Teor. Fiz. **9**, 609 (1969) [JETP Lett. **9**, 371 (1969)].
[48]Yu. P. Raĭzer, Lazernaya iskra i rasprostranenie razryadov (The Laser Spark and the Propagation of Discharges), Nauka, Moscow, 1974; Usp. Fiz. Nauk **132**, 549 (1980) [Sov. Phys. Usp. **23**, 789 (1980)].
[49]D. A. Frank-Kamenetskiĭ, Diffuziya i teploperedacha v khimicheskoĭ kinetike (Diffusion and Heat Transfer in Chemical Kinetics), Nauka, Moscow, 1967.
[50]Ya. B. Zel'dovich, G. I. Barenblatt, V. B. Librovich, and G. M. Makhviladze, Matematicheskaya teoriya goreniya i vzryva (Mathematical Theory of Combustion and Explosion), Nauka, Moscow, 1980.
[51]A. G. Merzhanov, V. V. Barelko, I. I. Kurochka, and K. G. Shkadinskiĭ. Dokl. Akad. Nauk SSSR **221**, 1114 (1975).
[52]Yu. E. Volodin, V. V. Barelko, and A. G. Merzhanov, Khim. Fiz. **1**, 670 (1982).
[53]A. G. Khachaturyan, Teoriya fazovykh perekhodov i struktura tverdykh rastvorov (The Theory of Phase Transitions and the Structure of Solid Solutions), Nauka, Moscow, 1974.
[54]V. V. Barelko and Yu. E. Volodin, Dokl. Akad. Nauk SSSR **223**, 112 (1975).
[55]Yu. V. Kopaev, Tr. Fiz. Inst. Akad. Nauk SSSR **86**, 3, (1975).
[56]E. B. Sonin, Usp. Fiz. Nauk **137**, 267 (1982) [Sov. Phys. Usp. **25**, 409 (1982)].
[57]I. M. Lifshitz, Zh. Eksp. Teor. Fiz. **12**, 117, 137, 156 (1942).
[58]I. M. Lifshitz and L. N. Rozentsveig, Zh. Eksp. Teor. Fiz. **18**, 1012 (1948).
[59]A. M. Kosevich, Fizicheskaya mekhanika real'nykh kristallov (Physical Mechanics of Real Crystals), Naukova Dumka, Kiev, 1981.
[60]Ya. I. Frenkel' and T. A. Kontorova, Zh. Eksp. Teor. Fiz. **8**, 1340 (1938).
[61]F. C. Frank and Yu. V. Kopaev, Usp. Fiz. Nauk **133**, 259 (1981) [Usp. Fiz. Nauk **24**, 116 (1981)].
[62]V. F. Elesin and Yu. V. Kopaev, Usp. Fiz. Nauk **133**, 259 (1981) [Sov. Phys. Usp. **24**, 116 (1981)].
[63]L. V. Keldysh, Vestn. Mosk. Univ. Fiz. Astron. **19**, No. 4, 86 (1978).
[64]Yu. D. Kalafati, I. A. Serbinov, and L. A. Ryabova, Pis'ma Zh. Eksp. Teor. Fiz. **29**, 637 (1979) [JETP Lett. **29**, 583 (1979)].
[65]A. N. Kolmogorov, I. G. Petrovskiĭ, and N. S. Piskunov, Byull. Mosk. Univ. Ser. Mat. Mekh. **1**, 6 (1937).
[66]Ya. B. Zel'dovich, Zh. Fiz. Khim. **22**, 27 (1948).
[67]I. M. Gel'fand, Usp. Mat. Nauk **14**, No. 1, 87 (1959).
[68]Y. Kametaka, Osaka J. Math. **13**, 11 (1976).
[69]L. D. Landau and E. M. Lifshitz, Elektrodinamika sploshnykh sred, Gostekhizdat, Moscow, 1958. (Engl. Transl., Electrodynamics of Continuous Media, Pergamon Press, Oxford (1960)).
[70]S. S. Kutateladze, Osnovy teorii teploobmena (Fundamentals of Heat Transfer), Atomizdat, Moscow, 1979.
[71]Heat Transfer at Low Temperatures, ed. by W. Frost, Plenum Press, N.Y., 1975 [Russ. Transl., Mir, Moscow, 1977].
[72]V. L. Ginzburg and A. V. Gurevich, Usp. Fiz. Nauk **70**, 201 (1960) [Sov. Phys. Usp. **3**, 115 (1960)].
[73]Yu. P. Raĭzer, Osnovy sovremennoĭ fiziki gazorazryadnykh protsessov (Fundamentals of the Modern Physics of Gas-Discharge Processes), Nauka, Moscow, 1980.
[74]F. G. Bass and Yu. G. Gurevich, Goryachie elektrony i sil'nye elektromagnitnye volny v plazme poluprovodnikov i gazovogo razryada (Hot Electrons and Strong Electromagnetic Waves in Semiconductor and Gas-Discharge Plasmas), Nauka, Moscow, 1975.
[75]L. D. Landau and E. M. Lifshitz, Mekhanika (Mechanics), Nauka, Moscow, 1973 [Engl. Transl. Mechanics, 3rd ed., Pergamon Press, Oxford (1976)].
[76]Bifurcation Theroy and Nonlinear Eigenvalue Problems, ed. by J. B. Keller and S. Antman, Benjamin, N.Y., 1969 [Russ. Transl., Mir, Moscow, 1974].
[77]O. V. Klyavin, V kn. Fizicheskie protsessy plasticheskoĭ deformatsii pri nizkikh temperaturakh (in: Physical Processes Accompanying Plastic Deformation at Low Temperatures), Kiev, 1974.
[78]V. I. Startsev, V. Ya. Il'ichev, and V. V. Pustovalov, Plastichnost' i prochnost' metallov pri nizkikh temperaturakh (Plasticity and Strength of Metals at Low Temperatures), Metallurgiya, Moscow, 1975.
[79]G. Dharmadurai, Phys. Status Solidi A **62**, 9 (1980).
[80]D. Bedeaux, P. Mazur, and R. A. Pasmanter, Physica (Utrecht) A **86**, 355 (1977); **90**, 151 (1978).
[81]D. Bedeaux and D. Mazur, *ibid.* **105**, 1 (1981).
[82]P. Mazur and D. Bedeaux, J. Stat. Phys. **24**, 215 (1981).
[83]A. A. Andronov, A. A. Vitt, and S. E. Khaĭkin, Teoriya kolebaniĭ (Theory of Oscillations), Nauka, Moscow, 1981.
[84]A. V. Gurevich and R. G. Mints, Dokl. Akad. Nauk SSSR **267**, 1103 (1982).
[85]I. I. Eru, S. A. Peskovatskiĭ, and A. V. Poladich, Fiz. Tverd. Tela (Leningrad) **15**, 2228 (1973) [Sov. Phys. Solid State **15**, 1488 (1974)].
[86]R. P. Huebener, J. Appl. Phys. **46**, 4982 (1975).
[87]V. N. Bogomolov, B. E. Kvyatkovskiĭ, E. B. Kolla, S. A. Ktitorov, Yu. A. Kumzerov, and N. M. Okuneva, Fiz. Tverd. Tela (Leningrad) **23**, 2173 (1981) [Sov. Phys. Solid State **23**, 1271 (1981)].
[88]V. A. Al'tov, V. B. Zenkevich, M. G. Kremlev, and V. V. Sychev, Stabilizatsiya sverkhprovodyashchikh magnitnykh sistem (Stabilization of Superconducting Magnetic Systems), Energiya, Moscow, 1975.
[89]V. P. Baev, A. V. Gurevich, R. G. Mints, and M. S. Ushomirskiĭ, Fiz. Tverd. Tela (Leningrad) **24**, 1544 (1982) [Sov. Phys. Solid State **24**, 886 (1982)].
[90]H. A. Schafft, Proc. IEEE **55**, 1272 (1967).
[91]B. S. Kerner and V. V. Osipov, Mikroelektronika **6**, 337 (1977).
[92]J. J. Stoker, Nonlinear Vibrations in Mechanical and Electrical Systems, John Wiley, N.Y., 1950 [Russ. Transl., IL, Moscow, 1953].
[93]A. B. Vasil'eva and V. F. Butuzov, Asimptoticheskie razlozheniya resheniĭ singulyarno vozmushchennykh uravneniĭ (Asymptotic Expansion for the Solutions of Singulary Perturbed Equations), Nauka, Moscow, 1973.
[94]B. S. Kerner and V. V. Osipov, Dokl. Akad. Nauk SSSR **264**, 1366 (1982).
[95]A. A. Abrikosov, Zh. Eksp. Teor. Fiz. **32**, 1442 (1957) [Sov. Phys. JETP 1174 (1957)].
[96]P. G. De Gennes, Superconductivity of Metals and Alloys, Benjamin, N.Y., 1966 [Russ. Transl., Mir, Moscow, 1968].
[97]C. A. Sai-Halasz, C. C. Chi, A. Denstein, and D. N. Langenberg, Phys. Rev. Lett. **33**, 215 (1974).
[98]P. Hu, R. C. Dynes, and W. Naraganamurti, Phys. Rev. B **10**, 2786 (1974).
[99]A. I. Golovashkin, K. V. Mitsen, and G. P. Motulevich, Zh. Eksp. Teor. Fiz. **68**, 1408 (1975) [Sov. Phys. JETP **68**, 701 (1975)].
[100]V. M. Dmitriev and E. V. Khristenko, Pis'ma Zh. Eksp. Teor. Fiz. **29**, 750 (1979) [JETP Lett. **29**, 697 (1979)].
[101]Yu. M. Gal'perin and V. I. Kozub, Fiz. Tverd. Tela (Leningrad) **19**, 2765 (1977) [Sov. Phys. Solid State **19**, 1618 (1977)].
[102]V. Eckern, A. Schmid, M. Schmutz, and G. Schön, J. Low Temp. Phys. **36**, 643 (1979).
[103]I. Iguchi, Phys. Rev. B **16**, 1954 (1977).
[104]J. Fich, P. W. Eppelrein, M. Welte, and W. Eisenmerger, Phys. Rev. Lett. **38**, 919 (1977).
[105]R. C. Dynes, C. J. Naraganamurti, and J. B. Carno, *ibid.* **39**, 229 (1977).
[106]K. V. Mitsen, Fiz. Tverd. Tela (Leningrad) **21**, 3475 (1979) [Sov. Phys. Solid State **21**, 2007 (1979)].
[107]K. E. Gray and H. Willemsen, J. Low Temp. Phys. **31**, 911 (1978).
[108]G. M. Eliashberg, Zh. Eksp. Teor. Fiz. **61**, 1254 (1971) [Sov. Phys. JETP **34**, 668 (1972].
[109]A. G. Aronov and B. Z. Spivak, Fiz. Nizk. Temp. **4**, 1365 (1978) [Sov. J. Low Temp. Phys. **4**, 641 (1978)].
[110]A. G. Aronov, Yu. M. Gal'perin, V. L. Gurevich, and V. I. Kozub, Adv. Phys. **30**, 539 (1981).
[111]A. M. Campbell and J. E. Evetts, Critical Currents in Superconductors, [Russ. Transl., Mir, Moscow, 1975].
[112]V. L. Ginzburg, Dokl. Akad. Nauk SSSR **118**, 464 (1958).
[113]R. P. Huebener, Phys. Rep. **13**, 143 (1974).
[114]J. W. Breemer and V. L. Newhouse, Phys. Rev. **116**, 309 (1959).
[115]L. E. Musienko, V. I. Shnyrkov, V. G. Volotskaya, and I. M. Dmitrienko, Fiz. Nizk. Temp. **1**, 413 (1975) [Sov. J. Low Temp. Phys. **1**, 205 (1975)].
[116]A. M. Kolchin, Yu. G. Mikhaĭlov, N. M. Raĭnov, A. V. Rumyantseva, A. P. Smirnov, and V. N. Totubolin, Zh. Eksp. Teor. Fiz. **40**, 1543 (1961) [Sov. Phys. JETP **13**, 1083 (1961)].
[117]A. P. Smirnov, V. N. Totubolin, and I. S. Parshina, Zh. Eksp. Teor. Fiz. **49**, 117 (1965) [Sov. Phys. JETP **22**, 84 (1966)].
[118]V. P. Galaĭko, Zh. Eksp. Teor. Fiz. **68**, 223 (1975) [Sov. Phys. JETP **41**,

108 (1975)].
[119]W. J. Skocpol, M. R. Beasley, and M. Tinkham, J. Low Temp. Phys. **16**, 145 (1974).
[120]A. I. D'yachenko, V. Yu. Taranenkov, and V. V. Stupakov, Zh. Eksp. Teor. Phys. **82**, 1262 (1982) [Sov. Phys. JETP **55**, 734 (1982)].
[121]A. I. Larkin and Yu. N. Ovchinnikov, Zh. Eksp. Teor. Fiz. **80**, 2334 (1981) [Sov. Phys. JETP **53**, 1221 (1981)].
[122]Yu. N. Ovchinnikov, Zh. Eksp. Teor. Fiz **82**, 2020 (1982) [Sov. Phys. JETP **55**, 1162 (1982)]; **84**, 230 (1983) [**57**, 132 (1983)].
[123]I. V. Avilova, L. M. Biberman, V. S. Vorob'ev, V. M. Zamalin, G. A. Kobzev, A. N. Lagar'kov, A. Kh. Mnatsakanyan, and G. É. Norman, Opticheskie svoĭstva goryachego vozdukha (Optical Properties of Hot Air) Nauka, Moscow, 1970.
[124]V. L. Granovskiĭ, Elektricheskiĭ tok v gaze (Electrical Current in a Gas), ed. by L. A. Sen and V. E. Golant, Nauka, Moscow, 1971.
[125]G. Dharmadurai, Nuovo Cimento B**64**, 503 (1981).
[126]A. I. Vakser and Yu. G. Gurevich, Fiz. Tverd. Tela (Leningrad) **24**, 3000 (1982) [Sov. Phys. Solid State **24**, 1698 (1982)].
[127]B. S. Petukhov and S. A. Kovalev, Izv. Vyssh. Uchebn. Zaved. Energetika No. 4, 81 (1963).
[128]S. A. Zhukov, V. V. Barelko, and A. G. Merzhanov, Dokl. Akad. Nauk SSSR **242**, 1064 (1978); **245**, 94 (1979); J. Heat and Mass Transfer **24**, 47 (1980).
[129]G. I. Abramov, A. V. Gurevich, V. M. Dzugutov, R. G. Mints, and L. M. Fisher, Pis'ma Zh. Eksp. Teor. Fiz. **37**, 453 (1983) [JETP Lett. **37**, 535 (1983)].
[130]V. V. Boĭko, Yu. F. Podrezov, and N. P. Klimova, Pis'ma Zh. Eksp. Teor. Fiz. **35**, 524 (1982) [JETP Lett. **35**, 649 (1982)].
[131]Yu. N. Tszyan and I. I. Logvinov, Fiz. Nizk. Temp. **8**, 774 (1982) [Sov. J. Low Temp. Phys. **8**, 388 (1982)].
[132]V. G. Voronkov and N. N. Semenov, Zh. Fiz. Khim. **13**, 1695 (1939).
[133]S. A. Zhukov and V. V. Barelko, Khim. Fiz. **1**, 516 (1982).
[134]Handbook of Chemical Lasers, ed. by R. W. Gross and J. F. Bott, J. Wiley, 1976 [Russ. Transl., Mir, Moscow, 1980].
[135]B. V. Novozhilov and V. S. Posvyanskiĭ, Fiz. Goreniya Vzryva **9**, 225 (1973); **10**, 94 (1974).
[136]A. I. Golovashkin, V. F. Elesin, O. I. Ivanenko, K. V. Mitsen, and G. P. Motulevich, Fiz. Tverd. Tela (Leningrad) **22**, 105 (1980) [Sov. Phys. Solid State **22**, 60 (1980)].
[137]V. F. Elesin, Zh. Eksp. Teor. Fiz. **71**, 1490 (1976) [Sov. Phys. JETP **44**, 780 (1976)]; **72**, 365 (1977) [*sic*].
[138]A. F. Volkov, Zh. Eksp. Teor. Fiz. **60**, 1500 (1971) [Sov. Phys. JETP **33**, 811 (1971)].
[139]A. A. Bugaev, B. P. Zakharchenya, and F. A. Chudnovskiĭ, Fazovyi perekhod metall—dielektrik i ego primeneniya (The Metal-Dielectric Phase Transition and Its Applications), Nauka, Leningrad, 1979.
[140]B. S. Kerner and V. V. Osipov, Zh. Eksp. Teor. Fiz. **74**, 1675 (1978) [Sov. Phys. JETP **47**, 874 (1978)]; **79**, 2218 (1980) [**52**, 1122 (1980)].
[141]J. Ross and P. Ortoleva, J. Chem. Phys. **56**, 4397 (1972); **58**, 5673 (1973); **63**, 3398 (1975).
[142]E. K. Bimpong-Bota, A. Nitzan, P. Ortoleva, and J. Ross, J. Chem. Phys. **66**, 3650 (1977).
[143]P. Hanusse, J. Ross, and P. Ortoleva, Adv. Chem. Phys. **38**, 317 (1978).

Translated by S. Chomet